Characterization of Biochar for Use in Treating Copper (II) Polluted Stormwater

by
Joy-Marie Danielle Gerould

A THESIS

submitted to

Oregon State University

University Honors College

in partial fulfillment of
the requirements for the
degree of

Honors Baccalaureate of Science in Environmental Engineering
(Honors Associate)

Presented May 26, 2016
Commencement June 2016

AN ABSTRACT OF THE THESIS OF

Joy-Marie Danielle Gerould for the degree of Honors Baccalaureate of Science in Environmental Engineering presented on May 26, 2016. Title: Characterization of Biochar for Use in Treating Copper (II) Polluted Stormwater .

Abstract approved: _____

Jeffrey Nason

Recent studies have discovered that salmon, specifically juvenile Coho Salmon, have their olfactory senses inhibited by the presence of low concentrations of copper concentrations at very low concentrations. Much of this copper is deposited on roadways by car brake pads during their use. The copper is carried with stormwater into nearby waterways during rainfall events and placed into contact with salmon populations. Many different types of adsorbent materials are being investigated as possible methods to remediate the copper in stormwater before it reaches nearby waterways. Biochar, similar to granular activated carbon (GAC), is one of these adsorbent materials and can be made as a byproduct of bioenergy production, which makes it less expensive than many other adsorbents. Biochars can be made from various different feedstocks and under varying production conditions, allowing them to have a wide range of properties.

This study assesses six different biochars (hazelnut shells and Douglas fir feedstocks at 3 different pyrolysis temperatures) for their ability to adsorb copper and determines through characterization experiments which properties of the biochars are correlated to the best copper adsorption. Knowing which properties are important to the

biochar's ability to adsorb copper allows biochars to be tailored toward the real life application of remediating the copper polluted stormwater. Batch isotherm experiments were performed and the data was analyzed using Langmuir and Freundlich isotherms. For the copper concentrations relevant to stormwater remediation H700 (hazelnut shells at 700°C), H500, and D700 biochars performed the best. Copper adsorption was observed to increase with increasing pyrolysis temperature. The addition of natural organic matter (NOM) to mimic realistic stormwater conditions reduced the copper adsorption by the biochar due to the copper complexing with the NOM.

Other trends noted were that increased adsorption of copper onto biochars correlates to higher biochar pH, increased fixed carbon content, and higher surface area. Although increased surface area does correlate to improved adsorption of copper by biochars, it does not appear to be the determining factor as the Douglas Fir biochars had a higher surface area (SA) compared to the Hazelnut shell biochars, but did not adsorb the copper as well. Based off FTIR spectra results for the hazelnut chars, aliphatic hydrocarbons are the only functional group type present at all three of the pyrolysis temperatures in addition to being the only functional group measured in the H700 char. Further investigation is recommended into the functional group analysis to determine if a specific group is responsible for increased copper adsorption. Overall, the H500 and H700 biochars performed the best out of all six and it is recommended that these be used for any future testing related to implementing them in-situ to remediate stormwater.

Key Words: Biochar, Stormwater, Copper, Remediation, Salmon, Environmental, Adsorbent, Isotherm, Langmuir, Freundlich, FTIR, BET, Characterization

Corresponding e-mail address: joymariegerould@gmail.com

Characterization of Biochar for Use in Treating Copper (II) Polluted Stormwater

by
Joy-Marie Gerould

A THESIS

submitted to

Oregon State University

University Honors College

in partial fulfillment of
the requirements for the
degree of

Honors Baccalaureate of Science in Environmental Engineering
(Honors Associate)

Presented May 26, 2016
Commencement June 2016

Honors Baccalaureate of Science in Environmental Engineering project of Joy-Marie Danielle Gerould presented on May 26, 2016.

APPROVED:

Jeffrey Nason, Mentor, representing Environmental Engineering

Mark Dolan, Committee Member, representing Environmental Engineering

Sarah Burch, Committee Member, representing Water Resource Engineering

Toni Doolen, Dean, University Honors College

I understand that my project will become part of the permanent collection of Oregon State University, University Honors College. My signature below authorizes release of my project to any reader upon request.

Joy-Marie Danielle Gerould, Author

TABLE OF CONTENTS Page

LIST OF FIGURES

Figure Page

LIST OF FIGURES (continued)

Figure Page

LIST OF TABLES

Table Page

ACKNOWLEDGEMENTS

Thank you to Dr. Jeff Nason for agreeing to be my faculty mentor for this project and for all the valuable help he has given me. It has been a great pleasure working on this project with him over the past 4-5 years. Thank you to Sarah Burch for her assistance with experiments and for being on my thesis committee. Thank you to Dr. Mark Dolan for agreeing to be on my thesis committee. Dr. Mark Johnson for assisting me with creating the biochars and various experiments throughout the research. Dr. Nick Wannenmacher for his help with the BET surface area and TGA. All of the researchers in Dr. Nason's lab for their support. Thank you to Pete and Rosalie Johnson for providing the opportunity to participate in the Johnson Internship program that started my journey into research. Thank you to the Honors College for encouraging students to participate in research and for offering the Honors Experience Scholarship to students to allow them to work on research for their thesis over the summer. Thank you to the Chambers Environmental Research Fund for the DeLoach Work Scholarship that helped me finish all of my research last summer. Lastly, thank you to my friends and family for being so supportive of me this entire time, specifically, my mom for encouraging me to participate in research and my fiancé, Tom, who is the reason I was able to accomplish this thesis.

DEDICATION

In Loving Memory of My Mother

I dedicate this thesis to my mom who encouraged me to participate research and was delighted when I ended up loving it. Turns out that you were right as usual. You always believed in me no matter what and pushed me to try new things that were outside of my comfort zone. I would have not been able to do my thesis or finish my degree without you supporting me. I miss you more than anything else in the world and wish you could be here to see me accomplish my dreams.

1. INTRODUCTION

1.1. Background

As vehicle brake pads are used, copper and other metals are deposited onto the roadway on which the car is driving. When it rains, those dissolved metal particles wash into storm drains or directly into nearby waterbodies. In fact, deposition from car brake pads account for up to half of the copper that enters waterbodies in urban areas (Washington State Department of Ecology 2016). Salmon, especially juveniles that are exposed to concentrations of copper as low as 2 parts per billion (ppb) can have their olfactory senses impaired (Baldwin 2003). This can prevent them from being able to use their olfactory senses to alert them to predators nearby making them less likely to modify their behavior to draw less attention from predators. High copper concentrations in water where salmon are present could have serious negative repercussions on salmon populations in the Pacific Northwest and elsewhere in the country.

Many state governments are aware and concerned about this issue and are working with brake manufacturers to reduce the amount of copper and other metals in their brakes. Even though new brakes are expected to have phased out their use of copper in Washington by 2025, that unfortunately does not mitigate copper pollution from brake pads that are already in use and will continue to be for some time. Until copper is no longer deposited into waterways from stormwater runoff, research into possible remediation strategies for the copper is advantageous. To that end, this study focused on testing different adsorbents, specifically biochars, for use in removing copper from

stormwater and characterizing the biochars to understand which properties correlate to the best removal efficiencies.

Traditionally, granular activated carbon (GAC) has been used to treat heavy metals and both natural and synthetic organics in water treatment plants. However, it is also fairly expensive, which makes it cost prohibitive to use for in-situ remediation on the wide scale implementation that would be necessary to treat the roadway runoff. There is considerable interest in biochar for copper adsorption (along with other heavy metals) in this scenario as it is very versatile and potentially inexpensive as it is a by-product of thermally processing biomass. However, it is still a relatively new type of adsorbent when compared to the much more commonly used GAC and as a result, there is still much to be learned about it. Biochars, which were the adsorbents used for copper treatment in this research, can be created using various organic starting materials, or feedstocks, and procedures, therefore the resulting biochars have different final properties. Often, biochars are created as a byproduct of pyrolysis intended to create liquid biofuel which can be burned to generate electricity. This is often most cost effective if the biochar is made from organic material that will not have any other use, for instance hazelnut or walnut shells that would simply be thrown into a landfill after being processed.

1.2. Objectives

Based on a literature survey conducted, two feedstocks, hazelnut shells and Douglas fir wood chips, were chosen to undergo pyrolysis at three different temperatures in order to obtain a wide range of potential properties between the biochars. From there, this work can be broken up into two main experimental phases as follows:

1. Adsorption isotherm experiments conducted to evaluate the biochars' ability to remove copper from solution.
2. Characterization of the biochars to determine the properties correlated to increased copper adsorption.

Together, the results from these tests will shed light onto which feedstock properties and pyrolysis conditions would be optimal for creating a biochar that is very effective at adsorbing copper.

1.3. Approach

Six biochars were created in collaboration with the Environmental Protection Agency (EPA) using hazelnut shells and Douglas fir wood chips as feedstocks and were pyrolyzed at three different temperatures (300, 500, and 700°C). Once ground to the proper size, kinetics tests were performed on the biochars in synthetic stormwater solutions to determine the time for the copper to reach equilibrium between the solid and aqueous phases. Once that was determined, batch isotherm experiments were performed to evaluate the various biochars' ability to adsorb copper. Further testing was conducted with batch isotherms in the presence of natural organic matter (NOM) to more accurately replicate conditions that would be present in stormwater. These kinetics and batch isotherm experiments complete the first phase of the objectives for this work. The characterization of the biochar, which makes up the second experimental phase, consisted of the following procedures: biochar pH measurement; Brunauer, Emmett, and Teller (BET) surface area analysis; thermogravimetric analysis (TGA); proximate carbon analysis; and Fourier transform infrared spectroscopy (FTIR) analysis.

The remainder of this thesis contains five additional sections. Section 2 encompasses the relevant literature that was reviewed as a basis for this research including copper's effects on salmon, biochar as an adsorbent for copper, and correlations found in previous studies between biochar's ability to adsorb copper and its properties. Section 3 is the materials and methods section and contains all of the procedures used in the course of this research. Section 4 contains the results and discussion for all of the experiments performed. The conclusions drawn from the research and recommended future work is included in section 5. Lastly, section 6 contains all of the supplemental information obtained in the course of completing this thesis.

2. LITERATURE REVIEW

2.1. Copper in Stormwater Runoff and its Effects on Salmon

Copper is used in vehicle brake pads to dissipate heat generated from braking and help reinforce the structure of the brakes to make them more durable (Shaheen 1975). As the brakes are used, they deposit small amounts of copper onto roadways which can then be carried into nearby waterways when it rains. While the amounts deposited by individual vehicles are minimal, the cumulative effect of all of the cars traveling through one area has large repercussions. In the nearby Columbia and Willamette Rivers, the median copper concentrations found were 1 μg/L or part per billion (ppb) (Morace 2013). While this concentration is one thousand times smaller than the allowable limit of copper in drinking water set by the Environmental Protection Agency (EPA 2016c), the concentrations present in waterways spike following the influx of stormwater to levels that have been shown to be harmful to salmon. Studies have shown two major concerns with salmon exposure to copper: decreased immune response and loss of olfactory senses. This is a major concern for salmon populations in this area as coho salmon are classified as a threatened species in the Columbia River (RCO 2009). Additionally, stormwater sampled for copper at various other sites around Oregon, as well as California, have had median copper concentrations between 9.08 μg/L and 40.9 μg/L (Nason et al. 2012; Kayhanian et al. 2007). This much higher concentration of copper found in stormwater could cause copper concentrations in nearby waterways to spike during rainfall events.

Tests conducted by the EPA's Corvallis Environmental Research Laboratory, determined that juvenile coho salmon exposed to copper concentrations of 18.1 μg/L

for long periods of time (30 days) cause significant mortality when exposed to a bacterium that is harmless when the fish is not immune compromised (Stevens 1977). While salmon in the Willamette or Columbia rivers may be exposed to concentrations this high soon after the beginning of a rainfall event due to a phenomenon called 'first flush' when the majority of copper is being transferred to the rivers, they will not be exposed to it for the length of time found in this study. First flush refers to the initial surface runoff during a rainstorm that carries the highest concentrations of contaminants, including copper. They also concluded that, even at lower concentrations or shorter exposure times, the fish experienced higher stress on their body which could make them less able to adapt to changes in environmental conditions.

A study conducted (McIntyre et al. 2015) exposed juvenile coho salmon to copper concentrations of 0, 5, 10, and 20 μg/ L for 3 hours, which are conditions that could occur in the Willamette and Columbia Rivers, and then exposed the fish to olfactory cues that signaled a predator upstream. The typical prey response of salmon was exhibited by decreased swimming speed and often near motionlessness to avoid the predator's notice. However, for the salmon that were exposed to 20 μg/L copper, there were no behavioral changes demonstrated in the salmon when exposed to any predator cues. The lower concentrations of copper (5 & 10 μg/L) resulted in slight behavioral changes, but significantly less change than in unexposed salmon. The concern about the change in behavior of salmon exposed to even low concentrations of copper is that these salmon, especially juveniles, will be more likely to fall victim to predation. This could have dramatic effects on salmon populations in the

Willamette and Columbia Rivers as well any other area where salmon are exposed to high copper concentrations in water. Another study indicates that copper concentrations less than 10 ppb for short exposures of a few minutes to few hours could have similar results on the salmon (Baldwin et al. 2010). This effect in salmon applies to both hatchery raised and wild-reared coho salmon and could potentially have negative effects on steelhead salmon and other types of fish as well. While these effects have not been studied as much, steelhead, chinook, and chum salmon are considered threatened or endangered species (depending on the location) in both the Willamette and Columbia Rivers (RCO 2009; NMFS 2011).

One positive discovery is that the inhibition of the salmon's olfactory senses is reversible. After being exposed to copper concentrations high enough to cause olfactory inhibition (around 1 ppb), if the fish are then placed in water with lower or no detectable copper concentration, their olfactory senses gradually become functional again over a few hours (Wang et al. 2013).

2.2. Biochar Production

Biochar is class of materials encompassing the products of thermal treatment of biomass feedstocks (including charcoal) that can be used as a soil amendment or as an adsorbent in water treatment (USBI 2014). It can be created using two different methods: pyrolysis and gasification, both of which involve heating organic material (referred to as the feedstock) in a controlled and specialized kiln. Gasification is generally used to make small batches of biochars and can be done both in the presence and absence of oxygen. Pyrolysis is the more commonly used process for industrial applications and involves heating the feedstock up in the absence of oxygen

and capturing the organic gas created from the volatilization of aromatic compounds in the feedstock (IBI 2016a). This process produces both biochar (normally the

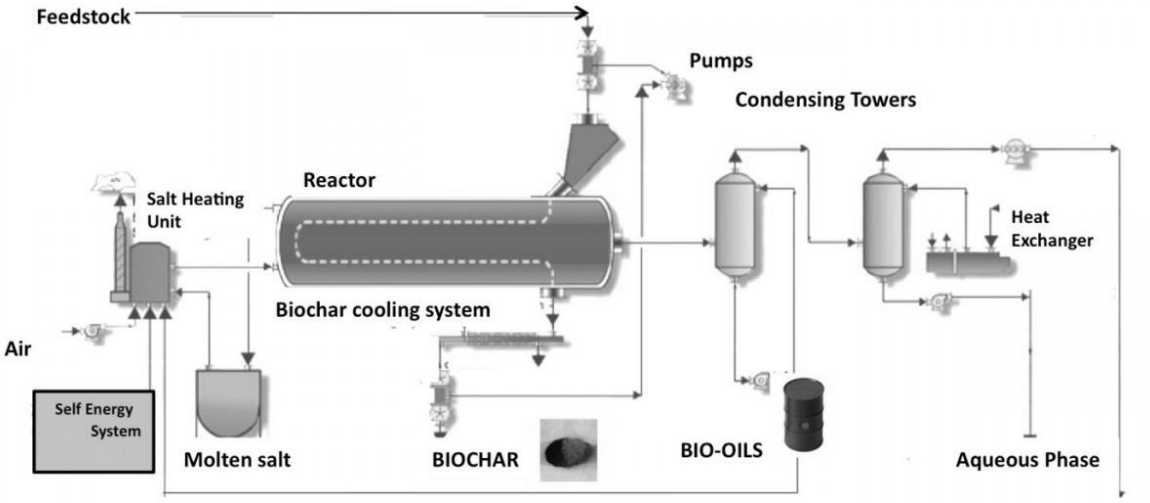

Figure 2.1-Schematic of pyrolysis kiln and bio-oil capture equipment. (IBI 2016b)

Gasification is a process similar to pyrolysis but produces syngas, or synthetic gas, instead of bio-oil in addition to the biochar by-product. Feedstocks are typically pyrolyzed at 300°C and above as most organics do not volatilize at lower temperatures. Most of the volatilization of organic material occurs between 300°C and 450°C (McBeath et al. 2015). Another study found that "as pyrolysis temperature increased, pH, ash content, carbon stability, and total content of carbon increased while biochar yield, volatile matter, and total content of hydrogen, oxygen, nitrogen, and sulfur decreased" (Zhang et al. 2014). These different relationships can help researchers create tailored biochars for specific applications. The type of feedstock used also has significant effect what properties the biochar will have and in turn what uses the biochar is best suited for.

2.3. Biochar as an Adsorbent for Aqueous Copper

Biochar has been typically used as a soil amendment (SOS, 2016), but has recently had additional attention for removal of heavy metals and organics from water or soil (Regmi et al. 2012; Tong et al. 2011; Zhang et al. 2014; Keiluweit et al. 2010; and Biniak et al. 1999). While the cost comparison between biochar and granular activated carbon (GAC) has not been conducted in relation to its use specifically as an adsorbent for copper, biochar has been shown to be a less expensive alternative to GAC for remediation of chromium, arsenic, and as an electrode material (Huggins et al. 2014; Mohan and Pittman 2007; Mohan and Pittman 2006). This can be attributed to relatively low cost of feedstocks used to produce the biochar and that biochar is often produced as a by-product of an already existing industrial process and does not undergo the steam or chemical activation step used to make GAC. Additionally, knowing which properties are important for the copper removal efficiency of the biochar can dictate how much the biochar costs to make due to the feedstock and pyrolysis process required. Many studies have also shown it to be more efficient at removal of heavy metals from water even though they generally do not undergo the steam activation step that makes GAC so porous. Links between higher surface area, higher fixed carbon content, and negative surface charge have all been shown to be properties that correlate to increased copper removal (Biniak et al. 1999; Tong et al. 2011; Zhang et al. 2014).

2.4. Adsorption Isotherms

The adsorption of an adsorbate onto an adsorbent, in this case copper (II) onto biochar, can often be described using one of two common different adsorption isotherm models- Langmuir or Freundlich (EPA 2016b). Figure 2.2 shows a

comparison between typical Langmuir and Freundlich isotherms (linear isotherms are a specific type of Freundlich isotherms).

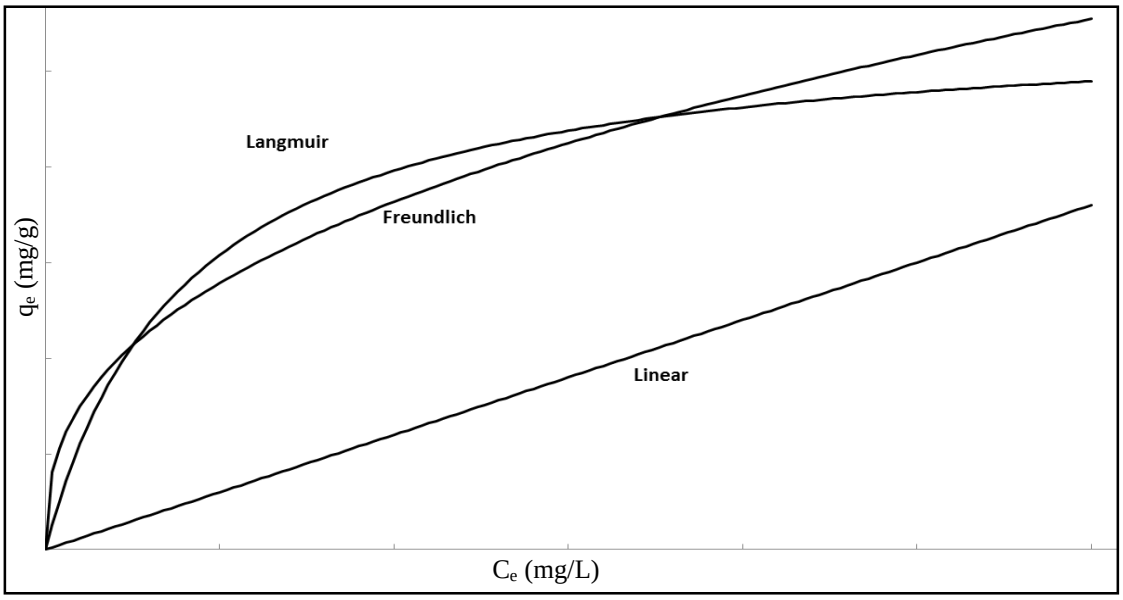

Figure 2.2-Typical Langmuir, Freundlich, and linear isotherm curves.

The assumption for the Langmuir isotherm is that there are a limited number of adsorption sites and that these sites are homogeneous (i.e., they have the same affinity for the adsorbate). The Freundlich isotherm is generally used when there are an unlimited number of surface sites but they all have different binding energies (heterogeneous sites).

Insight into the likely adsorption mechanism and characteristics of the adsorption sites on the biochar can be gained based on how well the collected data fits these models. The equation for Langmuir isotherm model is shown in equation 1 below,

(1)
$$q_e = \frac{q_{max} * K * C_e}{1 + (K * C_e)}$$

where q_e is the equilibrium loading concentration on the biochar (mg copper/g biochar), q_{max} is the maximum adsorption capacity limit (mg copper/g biochar), C_e is the aqueous phase equilibrium concentration of copper (mg copper/L solution), and K

is the relative energy of adsorption (L solution/ mg copper). The magnitude of the variable *K* quantifies the relative affinity that a given solute has for surface adsorption in that the larger the *K* value is, the higher affinity the adsorbent has for the adsorbate. Both q_{max} and *K* can be found empirically by linearizing the plotted data and then using the linear expression of the isotherm equation to determine those Langmuir constants. For the Langmuir isotherm, this is accomplished by plotting C_e/q_e vs C_e and creating a linear trendline for the plotted data. The equation that describes the trendline is used to find initial estimates for q_{max} and *K* and the R^2 value for the trendline shows how well the trendline and isotherm model fits the data collected. The linear expression (equation 2) is written as shown below to mirror the traditional linear equation form of y = mx + b.

(2) $$\frac{C_e}{q_e} = \frac{1}{q_{max}} C_e + \frac{1}{K q_{max}}$$

The slope of the linear trendline is the value for $1/q_{max}$ and the y-axis intercept is represented by $1/Kq_{max}$.

For the Freundlich model (equation 3), K_f is the constant used to describe the adsorption capacity and *n* is what describes the adsorption intensity and represents the degree of nonlinearity between the solution concentration and adsorption.

(3) $$q_e = K_f * (C_e)^{1/n}$$

Having a *1/n* value greater than 1 implies unfavorable sorption and only occurs at high adsorbate concentrations, whereas a 1/n value less than 1 implies favorable sorption (Desta 2013). A 1/n value equal to 1 is a special type of Freundlich isotherm known as a linear isotherm. A linear isotherm is written as shown below in equation 4.

(4) $$q_e = K_f * C_e$$

The equation representing the Freundlich isotherm linear trendline is used to determine the initial estimates for the isotherm constants *n* and K_f with the slope representing *1/n* and the y-intercept representing log (K_f). The linearized form of this equation is shown by equation 5.

(5) $$\text{Log}\, q_e = \log K_f + \frac{1}{n}(\log C_e)$$

The Non-Linear Least Squares Regression method is commonly used to estimate model parameters for Freundlich and Langmuir isotherm constants (Osmari et al. 2013; Armagan and Toprak 2013). Those initial estimates of isotherm parameters, along with the measured equilibrium aqueous copper concentration (C_e), are used to calculate q_e. The difference between q_e calculated from the initial guesses (referred to as q_{ecalc}) and the q_e obtained from the mass balance on the experiemental data (referred to as $q_{e\ experimental}$) is calculated and squared. This difference between these is the squared error, or SE, and is shown in equation 6.

(6) $$SE = \left(q_{e_{calc}} - q_{e_{experimental}}\right)^2$$

All of the squared errors are summed (referred to as sum of square errors or SSE) and are this value is minimized by changing the isotherm constants. The isotherm constants that create the smallest SSE are the final values used for the parameters for each biochar (Ncibi 2007; Osmari et al. 2013; Desta 2013, Ho et al. 2005).

2.5. Biochar Experimental Characterization Procedures

Multiple different techniques can be used to characterize the physical and chemical properties of biochar including thermogravimetric analysis (TGA), surface area, proximate carbon analysis, pH of biochar slurries, and Fourier transform infrared

spectroscopy analysis (FTIR). These specific experiments were chosen due to the frequency in which they appear in literature as methods for biochar characterization. (Chen et al 2011; Regmi et al. 2012; Tong et al. 2011; Zhang et al. 2014; Biniak et al. 1999; Kim et al. 2012; Manya 2012). The surface area of biochar is important because high surface area has been shown to increase biochar's ability at adsorption (Chen et al. 2011). Thermogravimetric analysis is performed on feedstocks to determine at what temperature different organics in the feedstocks volatilize and can determine the percent composition of the feedstock by weight (AMEI 2016). A sample TGA curve performed on a polymer can be seen below in Figure 2.3.

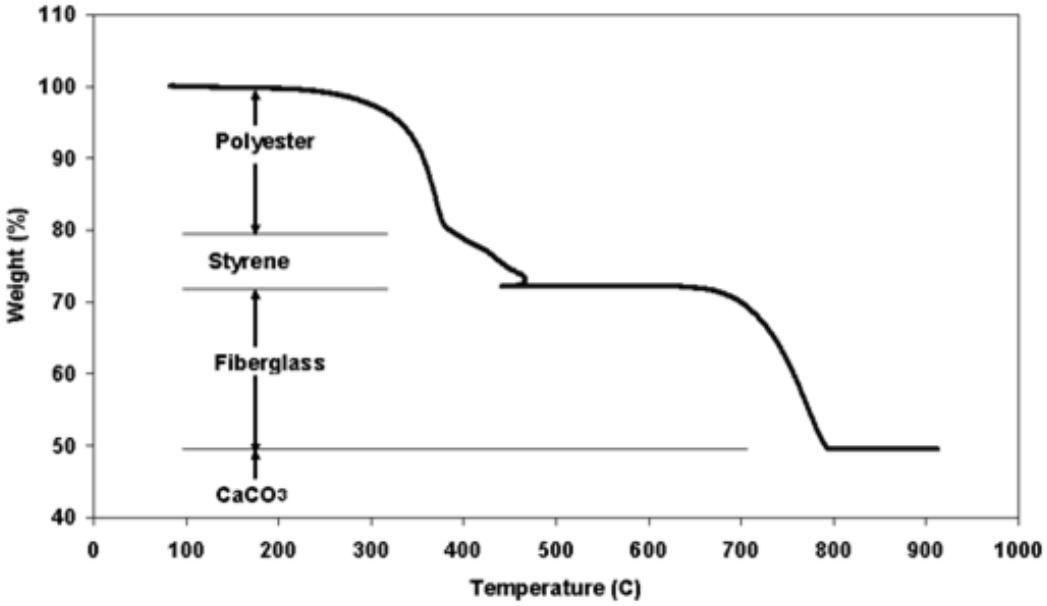

Figure 2.3-Thermogravimetric analysis conducted on an unidentified polymer (AMEI, 2016).

As the TGA temperature increases over the duration of the experiment, weight loss of the biochar is predominantly due to release of moisture and the volatilization of organics. A more stable form of carbon remains at the higher temperatures (Kim et al. 2012).

Proximate carbon analysis is performed to determine the amount of fixed carbon, ash, and volatiles present in the biochar. It has been suggested that biochars with higher ash content do not perform as well for copper removal while chars with high fixed carbon perform better (Brewer 2012). Adsorption experiments have also evaluated the effect that the solution pH has on the adsorption of copper and found that "adsorption capacity increased with increating pH until it plateaued at pH 5" (Chen et al. 2011). This high adsorption plateau persisted from pH 5-10 at which point the adsorption decreased again (Regmi et al. 2012). Biochar slurries that are measured to have pHs in the range of 5-10 will likely see increased adsorption over biochars with pH measurements lower than 5 or higher than 10. Lastly, FTIR analysis is performed on biochars to determine exactly which functional groups are present on the biochar and to determine correlations between the presence of specific functional groups and increased copper adsorption (Regmi et al.2012; Mukherjee et al. 2011).

3. MATERIALS AND METHODS

3.1. Biochar Production

All of the biochars used in the experiments included for the purpose of biochar characterization were made in cooperation with the Environmental Protection Agency office in Corvallis, Oregon with the help of Dr. Mark G. Johnson. Two different feedstocks provided by the EPA (hazelnut shells and Douglas fir wood chips) were chosen to undergo pyrolysis at varying conditions to make the biochars. Figures 3.1a and 3.1b below show the feedstocks prior to any processing done as part of the thesis.

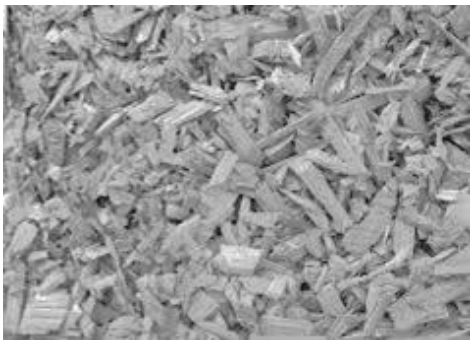

(a)

(b)

Figure 3.1- Both feedstocks were provided by the EPA for use on this project. **(a)** This image shows Douglas fir wood chips that could be made into biochar. **(b)** This image shows hazelnut shells that can be used as feedstock.

Both feedstocks were ground using the mill pictured in Figure 3.2 prior to undergoing pyrolysis to create a more uniform particle size as well as to allow the feedstocks to fit inside the crucibles that were used in the drying and pyrolysis steps.

Figure 3.2-Coarse (particle size) mill used to grind feedstocks at EPA

For the drying step, both feedstocks were placed in separate crucibles. These crucibles are shown in Figure 3.3.

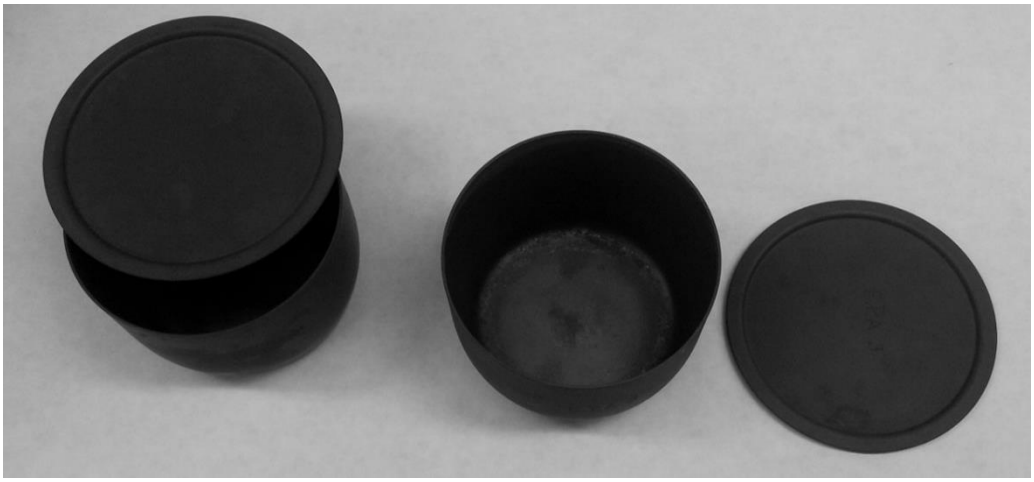

Figure 3.3-Large scale crucibles used to pyrolyzed feedstock into biochar.

The crucibles were placed in a pre-heated oven overnight at 105 °C with the lids slightly open to allow water vapor to escape the crucible. For the next step, each of the feedstocks were pyrolyzed at three different temperatures (300°C, 500°C, and 700°C), creating a total of 6 unique biochar batches. As an example, one of the batches, referred to as H700, was created by pyrolyzing the hazelnut shell feedstock at 700°C. Each of the crucibles containing feedstock was placed with the lids completely closed in the Thermo Scientific Lindberg Blue M™ Muffle Furnace

(shown in Figure 3.4) at the desired temperature for one hour in a N_2 atmosphere. Once that hour was up, the crucibles now containing biochar were removed and allowed to cool before weighing.

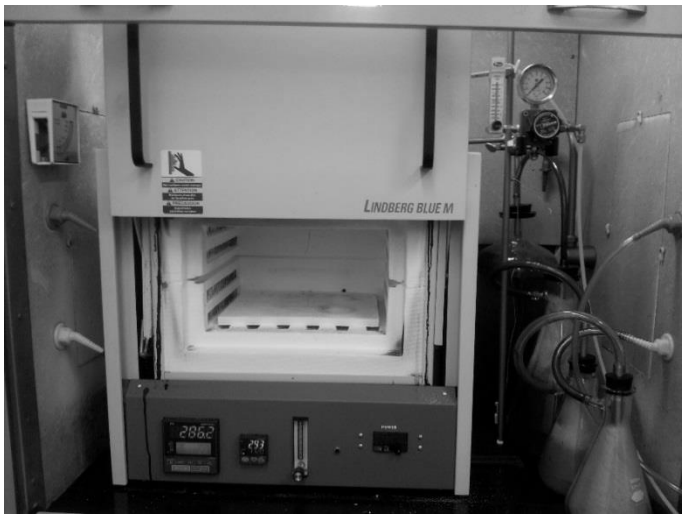

Figure 3.4- The muffle furnace used to create the biochars.

The biochars were designated according to their feedstock material and pyrolysis temperature and the notation for the different biochars is shown in Table 3.1.

Table 3.1- Biochar designations based on the feedstock and pyrolysis temperature.

Feedstock	Pyrolysis Temperature	Biochar Designation
Hazelnut Shells	300°C	H300
	500°C	H500
	700°C	H700
Douglas Fir Wood Chips	300°C	D300
	500°C	D500
	700°C	D700

The biochars were then ground up individually with a mortar and pestle and sieved to 40-50 mesh size shown in Figure 3.5, which was used for all further experimentation. 40-50 mesh size was defined as the biochar particle size that can pass through the 0.0165 inch opening of a 40 mesh sieve but cannot pass through the 0.0117 inch

opening of a 50 mesh sieve. For the purpose of this research, fines were defined as any biochar particles that were able to pass through the 50 mesh sieve and therefore have a diameter smaller than 0.0117 inches.

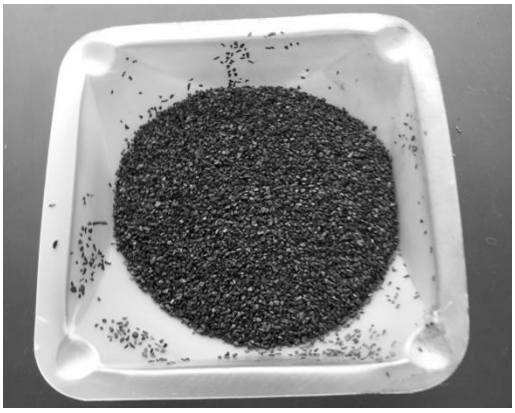

Figure 3.5- H700 biochar ground and sieved to 40-50 mesh size.

3.2. Batch Tests

3.2.1. Synthetic Stormwater

All of the batch tests (both kinetic and isotherm) used a synthetic stormwater mixture as the solution into which the biochar was placed. The solution was made up of 1 mM of NaCl, 0.185 mM $NaHCO_3$, and a varying concentration of copper but within the range of 0-1500 parts per billion (ppb). This solution was always adjusted to a pH of 6.0 ± 0.1 using 1.56 M HNO_3 and 3 M NaOH before the biochar is added to the 125 mL high density polyethylene (HDPE) bottles.

3.2.2. Kinetic Tests

Kinetics tests were conducted using both small and large scale batch procedures on the biochars to find the time required for the copper to reach equilibrium in aqueous and adsorbed phases. For the small-scale batch kinetics tests, only four of the six biochars were tested due to a limited quantity of the D700 and D500 biochars. Two different initial copper concentrations were used as part of the test- 500 and 1000 ppb.

The copper and synthetic stormwater solutions were made in 1 L volumetric flasks. Each of the 125 mL HDPE bottles contained 100 ± 5 mL of synthetic stormwater with the desired concentration of copper and 50 ± 1 mg of 40-50 mesh size biochar. Samples were taken at the times shown in Table 3.2. All times refer the time elapsing after the experiment began, which was defined as the time when the biochar was added to the HDPE bottles.

Table 3.2- Sampling times for batch kinetic tests of copper adsorption to biochar.

Sample	Time
1	0 hr
2	15 min
3	30 min
4	45 min
5	1 hr
6	2 hr
7	4 hr
8	8 hr
9	12 hr
10	24 hr
11	48 hr

All sample bottles (with the exception of the first sample taken at the beginning of the experiment) were placed in a tumbler to ensure thorough mixing of the biochar and stormwater solution. Once the designated time of reaction for each sample (shown in Table 2) was reached, the sample was removed from the tumbler and filtered into an ICP vial using a 45 μm Millipore vacuum filter in a standard vacuum filter set-up. The filtration apparatus was rinsed and dried after each sample. The pH of the sample was measured immediately after filtration using a Fisher Scientific accumet pH probe. The samples were acidified by adding 10 μL 70.0% assay ultrapure nitric acid (HNO_3) to each of the ICP vial samples and were refrigerated until they could be

analyzed. Copper concentration was analyzed using the inductively coupled plasma optical emission spectroscopy, or ICP-OES. The ICP-OES used had a detection limit of 0.5 ppb for copper.

The large-scale kinetics test was conducted twice, in which 0.5 g of H700 biochar was placed into 1 L of the synthetic stormwater with 500 ppb of copper. Unlike with the small batch kinetics tests, all samples were taken from the 1 L HDPE bottle and filtered with the sample bottle being placed back in the tumbler after each sampling and the test lasted 72 hours instead of 48 hours. The samples were filtered using the same procedure and experimental set-up as the small-scale batch samples. The samples had the pH measured immediately after filtering and followed the same acidification and storage procedure.

3.2.3. Synthetic Stormwater Batch Isotherm Tests

The batch isotherm tests followed a procedure very similar to the batch kinetics tests; however, each copper concentration was run in triplicate for this experiment and a larger number of copper concentrations were tested. The stormwater solutions were created following the procedure noted in section 3.2.1 Synthetic Stormwater. All six of the biochars and Calgon F-400 GAC underwent batch isotherm testing. The following initial copper concentration solutions were used for every biochar: 75 ppb, 150 ppb, 300 ppb, 500 ppb, 700 ppb, 900 ppb, 1100 ppb, and 1500 ppb. Additionally, only 80 mL of synthetic stormwater solution with copper and 40 mg of biochar was used for each 125 mL HDPE bottle sample. After the solution and biochar were added to the HDPE bottles, they were placed in the tumbler shown in Figure 3.6 for 48 hours as determined by the kinetics tests.

Figure 3.6- The tumbler used for the batch kinetics and isotherm tests is stored in Merryfield Hall.

The tumbler was used to ensure constant exposure of the biochar to copper in solution and prevents the biochar from settling to the bottom of the bottle. Once the 48 hours of the test duration had elapsed, the bottles were removed from the tumbler and vacuum filtered in order from lowest initial concentration to highest. The filtration procedure was slightly different from that used in the kinetics tests in that each of the samples run at the same initial copper concentration in triplicate used the same Millipore vacuum filter. These were only changed once a new initial copper concentration sample was being filtered at which point the vacuum filtration set-up up was also rinsed and dried. This was done to prevent dilution in between triplicate samples. As with the other batch experiments, the samples were acidified with 10 μL of ultrapure HNO_3 and stored in the lab refrigerator until they could be analyzed using the ICP-OES. Samples of each of the initial copper concentrations were taken and tested using the ICP as well. The final copper concentration data was fit to several potential isotherm equations as discussed in the results section.

3.2.4. Synthetic Stormwater with SRNOM Batch Isotherm Tests

Additional batch testing was conducted on the two biochars, H700 and H500, which were determined to be the most promising based on the initial synthetic stormwater testing. These tests were run using the same synthetic stormwater copper concentrations and were prepared according to the same procedure described above with the exception of adding Suwanee River Natural Organic Matter (SRNOM). Adding SRNOM to the stormwater simulates the effect that organic material present in stormwater runoff has on copper (II) adsorption. As a result, it could be determined how organic matter affected biochar's ability to adsorb copper. The SRNOM solution was made by adding 0.0250g of dry SRNOM powder and around 200 mL of nanopure distilled de-ionized (DDI) water to a 250 mL volumetric flask, adjusting the pH to 4.0 ± 0.1, and then filling the volumetric flask up to the 250 mL line with DDI water. This solution was then mixed consistently in the dark for 24 hours. The concentration of the SRNOM was tested using 3 samples (1: 20 dilution of the SRNOM solution in the 250 mL volumetric flask). The synthetic stormwater with SRNOM solutions contained 2.8 mg/L of SRNOM in addition to the other components that are in the synthetic stormwater solution discussed previously. The remainder of this experiment followed the same procedure as the synthetic stormwater equilibrium batch tests that were conducted without SRNOM and are described above.

3.3. Biochar Surface Area

The surface area of each biochar sample was measured on a MICROMERITICS ASAP 2020 using the Brunauer, Emmett, and Teller (BET) method. First, the empty sample tube, Styrofoam donut, and cap were weighed. Then a small amount of the

biochar (40-50 mesh size) was added and weighed. All of the measurements were performed numerous times to ensure accuracy. Then, the sample tube was placed in the degassing port, heated to 250ºC and degassed. Once that was finished, everything was re-weighed and put in the analysis port. Liquid nitrogen was poured into both of the containers (known as cold trap Dewars), which keep possible contaminants from interfering with the experiment. Throughout the entire analysis phase, N_2 gas is added to the degassed sample tube and at lower partial pressures, it adsorbs onto the chars. The surface area is obtained calculated sing the difference between the how much N_2 has is needed to cover the known surface area of the degassed sample tube and the amount needed to fill the degassed sample tube containing the biochars. Once the analysis had completed, the sample tube and all the contents were re-weighed for the final time.

3.4. Biochar pH

Biochar pH was measured using ISO 10390 (Soil Quality--Determination of pH) (ISO, 2005). Biochar fines (diameter < 0.0117 inch) were added to 0.01 M $CaCl_2$ solution in a 1:5 volume ratio. For each of the samples (run in duplicate), five mL of biochar and 25 mL of 0.01 M $CaCl_2$ solution were measured out separately in a graduated cylinder and combined into 125 mL HDPE bottles. The sample bottles were then placed into the tumbler that was used for the kinetics and isotherm experiments for 24 hours. At the end of the 24 hours, the pH of the solutions in the HDPE bottles were measured using a Fisher Scientific accumet pH probe while the sample bottles were being stirred with a magnetic stir bar on a stir plate.

3.5. Thermogravimetric Analysis

Thermogravimetric analysis, or TGA, was conducted using the same Douglas fir wood chips and hazelnut shell feedstocks (ground in the EPA mill) that were used to make the biochars. The feedstocks were then heated up at a rate of 2°C per minute using a Q500 machine manufactured by TA instruments and stored at the EPA. The temperature, time from the beginning of the experiment, and the weight percent remaining compared to the original weight were recorded in a spreadsheet.

3.6. Proximate Carbon Analysis

The proximate carbon analysis had multiple different steps and was used to determine the mass percentage of the biochar composition that was ash, volatile matter, and fixed carbon. First, the crucibles with their lids (similar to those used in the actual biochar production but smaller and shown in Figure 3.7a and 3.7b) were weighed.

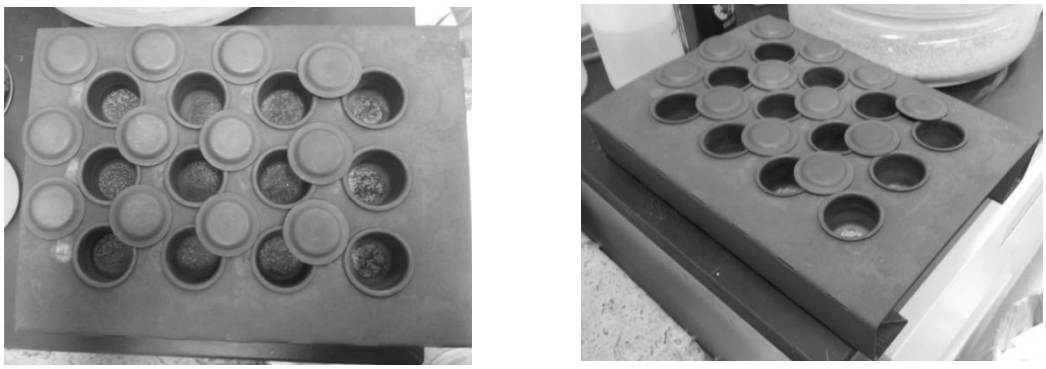

(a) (b)

Figure 3.7- Crucibles used for proximate carbon analysis. (a) ash content remaining in the crucibles after heating at 750°C for 6 hours. (b) This image shows the crucibles after the same step as shown in Figure 3.7a but at a different angle.

Then, each of the biochars were put into the crucibles (run in triplicate) and the crucibles were put into the oven at 105°C overnight with the lids slightly open, allowing any water vapor to escape the crucibles. Once this was completed, the crucibles were weighed with the lids and put into a Thermo Scientific Muffle Furnace

Lindberg Blue M™ for 6 minutes at 950°C with the lids closed. They were then taken out of the oven and allowed to cool before re-weighing the crucibles, lids, and char inside. The mass percent lost during the time in the furnace at 950°C was the volatile matter percentage. The crucibles were placed back into the muffle furnace at 750°C with no lids for 6 hours and then taken out and allowed to cool. The crucible and char were weighed and the mass lost during this phase was used to calculate the percentage of the biochar composition that was fixed carbon. The final mass of the biochar after the 6 hours at 750°C represents the portion of the biochar that was ash.

3.7. Fourier Transform Infrared Spectroscopy

For this portion of the research, fines of each of the biochars and Calgon F-400 granular activated carbon (GAC) were analyzed using the Thermo Nicolet machine picture in Figure 3.8 below.

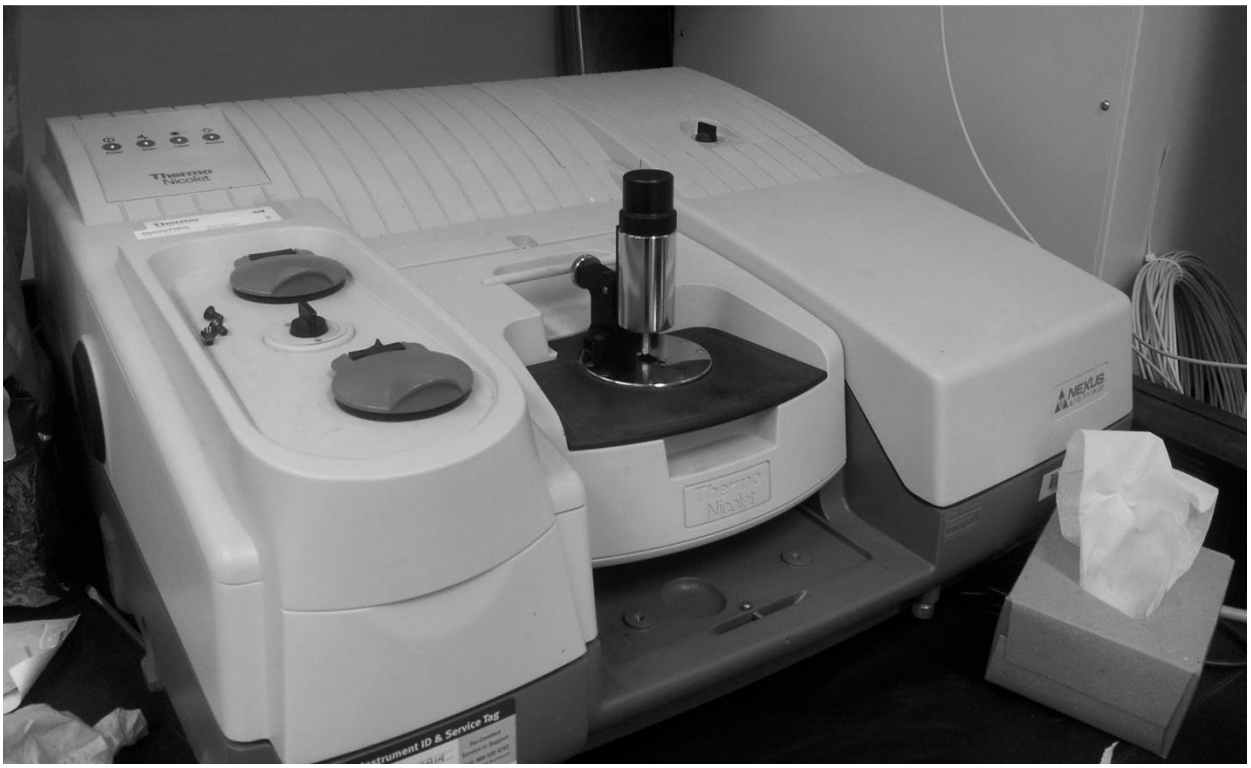

Figure 3.8- Thermo Nicolet FTIR machine housed at the EPA.

Once the machine was calibrated, minute amounts of the biochars were placed onto the glass above the laser (radiation source) and the data was measured using the detector and recorded by the attached computer. After each sample was analyzed, the glass above the laser was rinsed with ethanol and wiped down with a Chemwipe. The software corrected the baseline to include only relevant peaks and normalized the data to one for easier viewing and analysis. The IR Spectral interpretation software determined functional groups based off the wavenumber range of absorbance peaks. The D700, H700, and GAC were run multiple times as too much absorbance was recorded by the machine (caused by not enough light penetrating the adsorbents). Once the Thermo Nicolet was set to 40% sensitivity, some peaks were found for the chars.

4. RESULTS AND DISCUSSION

4.1. Adsorption Analysis

4.1.1. Kinetics Test Results

For all of the kinetic or isotherm batch tests, a calibration curve is used in conjunction with accurate copper concentration standards to calculate the copper concentrations present in the experimental sample solutions. The calibration curve for the ICP run that analyzed the H700, H500, H300, and D300 small batch kinetics tests is shown in Figure 4.1. The intensity of the copper in solution for each standard is measured by the ICP-OES and correlated to the copper concentration that is known to be in that standard (according to the way it was prepared).

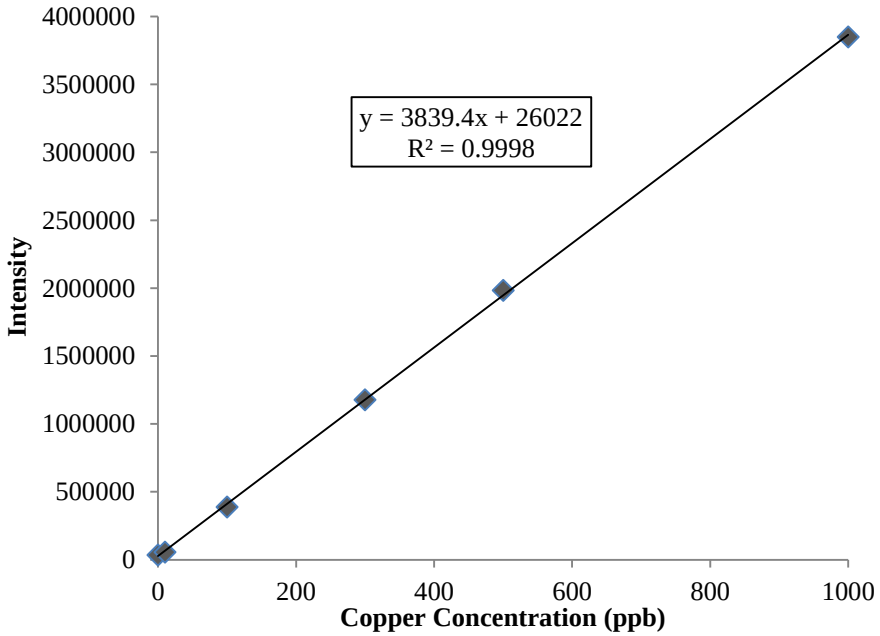

Figure 4.1- This calibration curve was generated using five standards (0 ppb, 10, 30, 500, and 1000 ppb copper).

A linear best-fit trendline is created using the data points on the graph and the equation displayed on the graph in Figure 4.1 represents the equation for the trendline. This equation allows the measured intensity for all the samples being tested

to be converted into copper concentrations. The R^2 value shown below the equation describes how well the linear trendline fits the data and the closer the value is to 1, the more accurate the trendline and equation. For this calibration curve, the R^2 value is 0.9998, which indicates that the trendline is a very good fit for the data collected.

The first set of batch tests conducted for both the 500 and 1000 ppb initial copper concentration in 125 mL bottles on H700, H500, H300, and D300 biochars showed significant fluctuation in copper concentration measured in the first 10 hours of the experiment. As noted earlier, the biochars used were all 40-50 mesh size to ensure that the equilibrium time would be valid for the planned batch isotherm experiments. Shown below in Figures 4.2, 4.3, 4.4, and 4.5 are the concentrations over time that were measured during this experiment. The dashed lines do not represent models or trendlines and are merely meant to make the order in which the data points were taken more apparent.

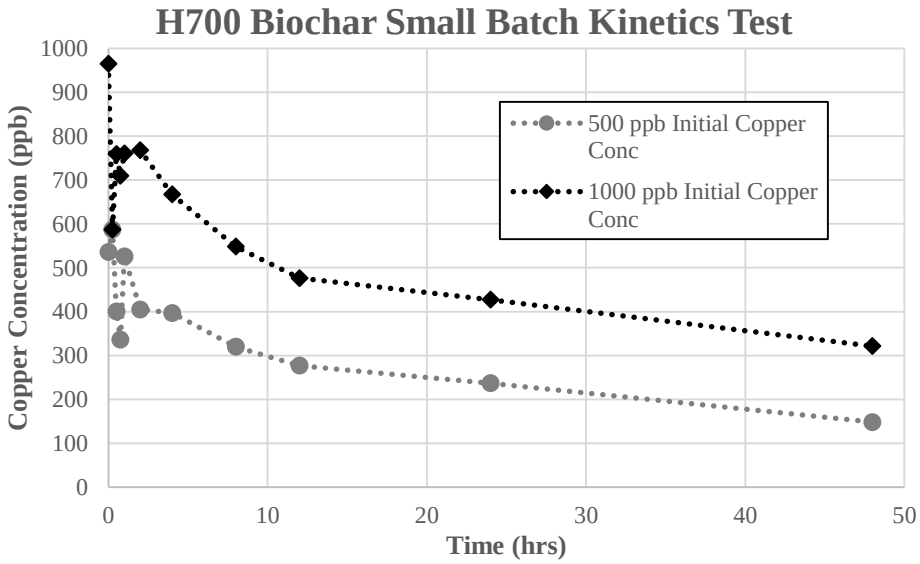

Figure 4.2-. Final measured concentrations at 48 hours were 148 ppb and 321 ppb for the 500 ppb and 1000 ppb initial copper concentrations respectively.

In both the H700 (Figure 4.2) and H500 biochar (Figure 4.3) small batch kinetics tests, while the rate of copper removal via adsorption by the biochar is decreasing, it is not clear if the copper concentration remains constant around 48 hours and thus reaches equilibrium or it continues to decrease after 48 hours.

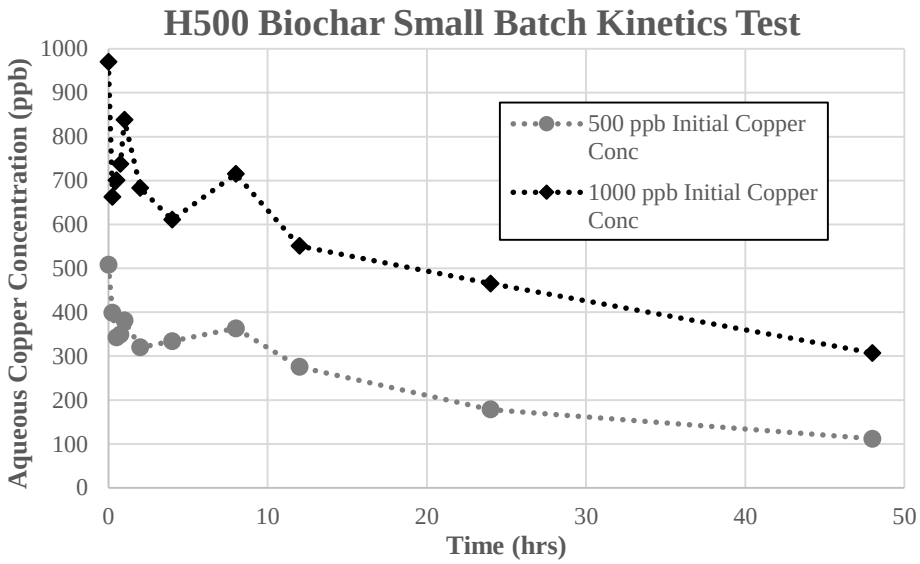

Figure 4.3- Final measured concentrations at 48 hours were 112 ppb and 306 ppb for the 500 ppb and 1000 ppb initial copper concentrations respectively.

For the H300 biochar kinetics tests, the lack of considerable change in copper concentration between the samples taken at 24 and 48 hours into the experiment denotes that the copper is in equilibrium between aqueous and solid (bound to the biochar) phases.

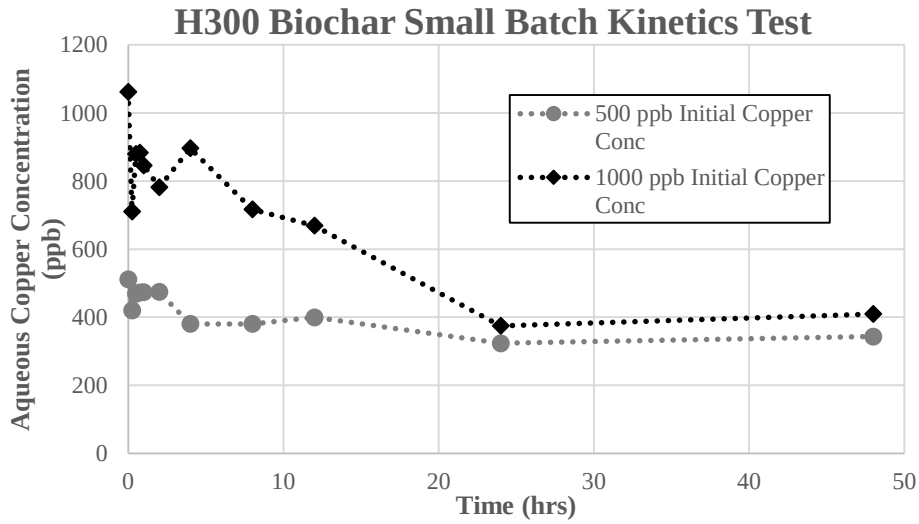

Figure 4.4- Final measured concentrations at 48 hours were 343 ppb and 409 ppb for the 500 ppb and 1000 ppb initial copper concentrations respectively.

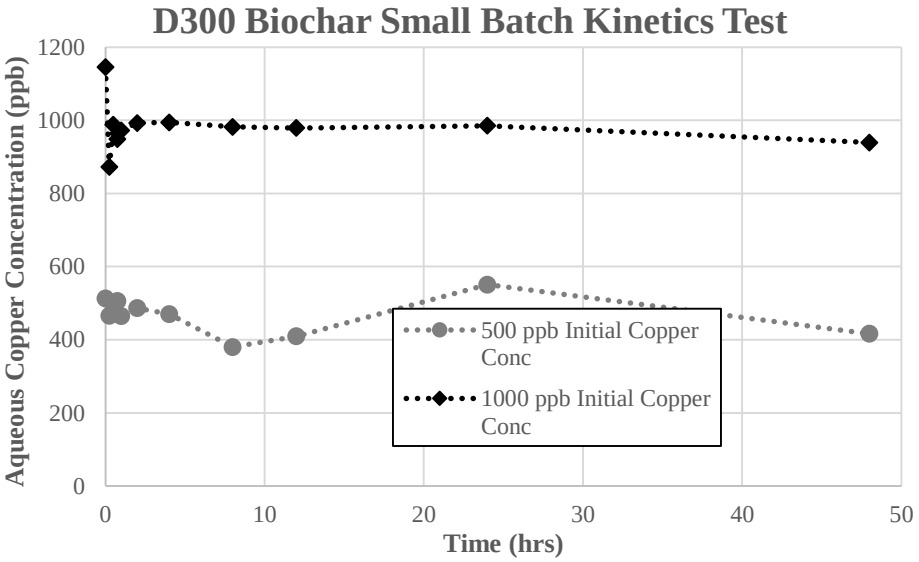

Figure 4.5- Final measured concentrations at 48 hours were 416 ppb and 939 ppb for the 500 ppb and 1000 ppb initial copper concentrations respectively.

Compared to either of the three other biochars tested during this experiment, the D300 biochar copper concentrations fluctuate much less during the first 10 hours of the test. It also appears to plateau more during the 24-48 hour phase than either the H500 or H700. A comparison of final concentrations between the biochars at 48 hours show that the H700 and H500 biochars have fairly similar final concentrations for both of the initial concentration data sets. The H300 biochar has half the copper

removal of either the H700 or H500 chars at 48 hours for the 500 ppb copper initial concentration data set. The D300 biochar removed almost no copper from either the 500 or 1000 ppb initial copper concentrations.

Overall, the results for all 4 biochars tested were fairly inconclusive as to whether the biochars reach equilibrium at 48 hours since there were no samples taken after that time to confirm the predicted concentrations. Based on this data, the H500 and H700 chars still appear to be adsorbing copper at a significant rate at 48 hours into the test. As there was more of the 40-50 mesh size required for this experiment of the H700 char, further testing was conducted using the large batch kinetics test described in the material and methods section. Additionally, this large batch kinetics test procedure was chosen to potentially reduce the amount of fluctuations measured during the first 10 hours of the experiments. Two trials of the H700 biochar were run at an initial copper concentration of 500 ppb for a total of 72 hours.

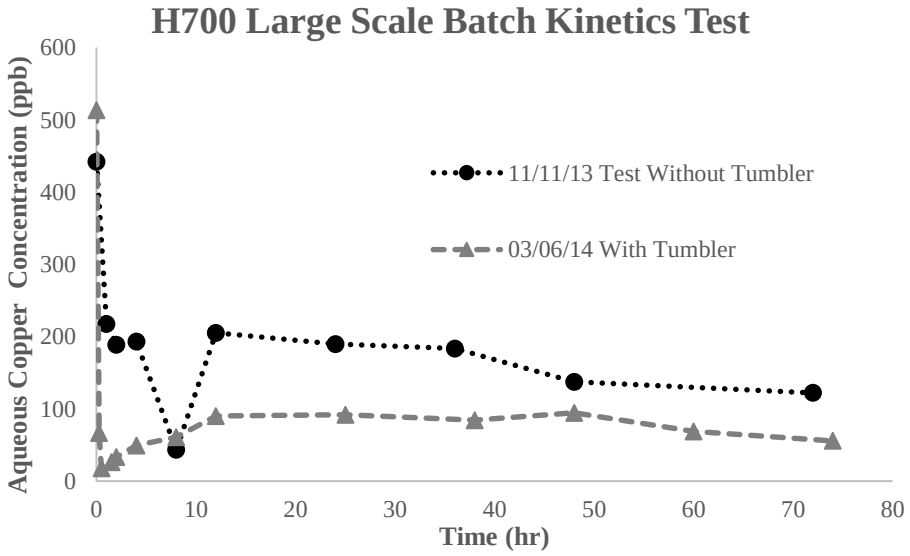

Figure 4.6-Large batch scale kinetics test conducted on the H700 biochar at an initial copper concentration of 500 ppb.

It is apparent that not having the tumbler operational for the 11/11/13 test dramatically decreased the amount of copper removed from aqueous form by the biochar. The faster reaction time (and shorter time to reach equilibrium-around 12 hours) in the data from the 03/06/14 test compared to the 11/11/13 test can likely be attributed to more thorough mixing due to the tumbler. The large decrease in concentration between 5-10 hours and then increase in concentration around 10-15 hours into the 11-11-13 test is similar to patterns in the small batch kinetics tests using D300 at 500 ppb, H300 at 500 ppb, and the H500 biochar at both initial concentrations during the same experimental time frame. This mirrors an increase in pH measured between 5-10 hours and then a decrease in pH after 10 hours into the test. The pH measured around 48 hours into the test is close to the pH measured during the increase at 5-10 hours. This can likely be attributed to copper quickly adsorbing to the chars from 5-10 hours and the desorbing some of the copper from 10-15 hours into the test and finally resorbing the copper and plateauing around 48 hours. pH values recorded during the kinetics tests can be found in the Appendix. However, the large-scale batch tests confirm that based on relatively constant copper concentrations from around 12 hours to 74 hours into the 03/06/14 test during which time the copper concentration only decreased by 34 ppb, that the mixture was at equilibrium during this time. So based on the experimental results, it was concluded that 48 hours in the tumbler after the biochar and stormwater solutions were mixed is sufficient time to reach equilibrium for any of the biochars that were part of this study.

4.1.2. Synthetic Stormwater Batch Isotherm Test Results

Once the samples were run through the ICP-OES, the data generated was used to calculate adsorption isotherms. The ICP records the final concentration of copper, C_e, in the aqueous phase and a mass balance can be performed based on that and the known initial concentration of copper in the solution to find the amount of copper adsorbed by the biochar as shown in Equation 7 below.

$$q_e = \frac{(V(C_i - C_e))}{M_B} \quad (7)$$

This equation describes the mass balance performed on the copper where q_e is the equilibrium loading on the biochar (mg copper/g biochar), V is the volume of the synthetic stormwater solution present in the HDPE bottle (L), C_i is the initial aqueous phase copper concentration (mg copper/L), C_e is the aqueous phase copper concentration at equilibrium (mg copper/L), and M_B (g biochar) is the mass of biochar placed into the HDPE bottle at the beginning of the experiment.

All of the copper adsorption data is analyzed using the linearization procedure (Linear Least Squares Regression) described in the literature review to determine initial estimates for the isotherm constants and to see which model best fits the data for each of the different biochars. Equations 2, 5, and 6 were used to calculate the final parameters displayed as part of the results. Initial values for each of the isotherms and biochars can be found in the appendix. The procedure of linearization of data to fit it to models was varied slightly between the two different isotherm models. For the Langmuir model, this entailed plotting the aqueous equilibrium concentration, C_e, on the x-axis and the calculated values for C_e/q_e (the ratio of aqueous equilibrium concentration to equilibrium loading on the biochar) on the y-axis. A linear trendline for this data was created and the R^2 of this trendline shows how well the data fits this

type of model. Figure 4.7 shows the linearized Langmuir isotherm for the experimental D500 biochar data.

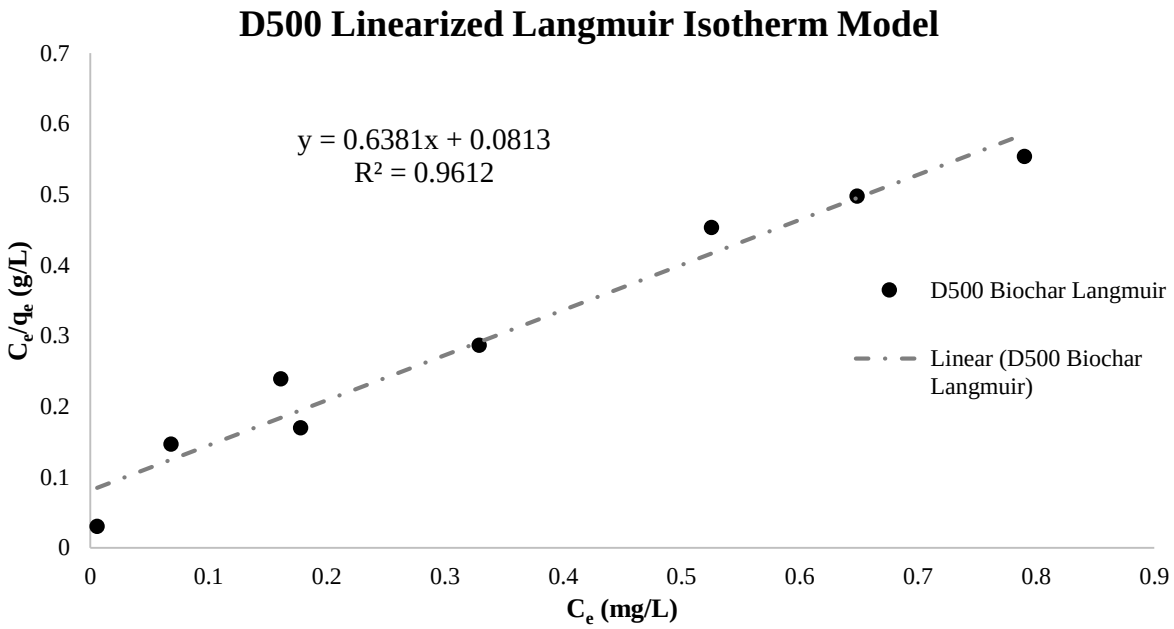

Figure 4.7-The graph above shows the linearized data for the D500 biochar for the Langmuir isotherm. The equation y = 0.6381x + 0.0813 represents the linear trendline and the R^2 value is 0.9612.

To model the linearized Freundlich isotherm, the log (C_e) was plotted on the x-axis and the log (q_e) on the y-axis. As with the Langmuir isotherm model, a linear trendline was also created and that R^2 value can be used to determine how well the data fits this model. Figure 4.8 shows an example of experimental biochar data, in this case for the D500 biochar, fitted to the linearized Freundlich model.

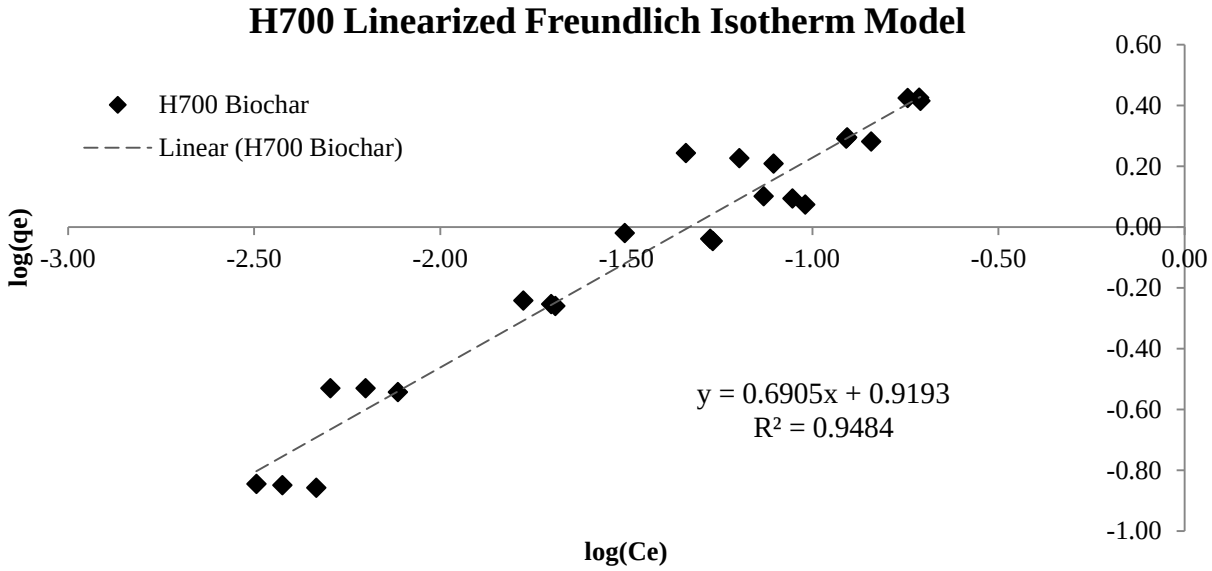

Figure 4.8- The graph depicts a linearized Freundlich isotherm for the H700 biochar data plotted as log (C_e) on the x-axis vs log (q_e) on the y-axis. The dotted trendline is described by the equation y = 0.6905x + 0.9193 with an R^2 value of 0.9484.

All of the R^2 values were modeled for both Langmuir and Freundlich using the experimental data from all six biochars and are shown in Table 7.1 in the appendix. Table 4.1 shows the constants that were calculated for both the Langmuir and Freundlich isotherms based on the linear trendline equation initial estimates and iterated using the Non-Linear Least Squares method to find the final values.

Table 4.1- Isotherm parameters for Langmuir and Freundlich isotherms determined through linearization of plotted data and the Least Squares Method.

Calculated Isotherm Constants			
Langmuir			
Biochar	**q_{max} (mg/g)**	**k (L/mg)**	***SSE***
D300	0.18	143.80	0.54
D500	1.62	6.32	1.01
D700	0.99	76.88	0.74
H300	0.73	9.86	0.72
H500	2.56	11.35	2.81
H700	4.50	6.42	1.55
GAC	1.26	18.06	0.41
Freundlich			
Biochar	**n**	**K_f**	***SSE***
D300	20.69	0.18	0.54
D500	2.62	1.55	1.05
D700	3.99	1.19	0.49
H300	2.92	0.73	0.66
H500	2.05	3.75	2.96
H700	1.57	7.34	1.31
GAC	0.506	2.12	0.43

No concrete conclusions about which isotherm model is a better fit for either the Douglas fir or hazelnut shell biochars can be drawn based on the comparison of SSE values for the Langmuir and Freundlich isotherms as the SSE values are very similar between the two models. This is likely because the initial copper concentrations that are high enough to display the plateau (where the amount of copper that is able to be adsorbed by the biochar levels out) were not tested in this study. The D300 biochar as modeled by the Freundlich isotherm has a significantly higher n value and much lower K_f value than any of the other biochars however, due to the extremely poor fit of the Freundlich model to the data collected for that biochar, no usable conclusions can be drawn from this. All of the biochars have *n* values such that their *1/n* is less

than 1, so it is favorable for the copper to sorb onto the biochars. As the data collected only had a few low initial copper concentrations, there may not be enough information to obtain good estimates of the isotherm constants. Using the calculated Langmuir model constants, while the D300 and D700 had the highest *K* values, they also have the lowest and third lowest q_{max} values. This means that while those biochars have a high affinity for copper, they are only able to adsorb a small amount of it before all the available sites for binding the copper on the biochar are occupied. Of all of the biochars (modeled using the Langmuir isotherm), the H700 char has the highest q_{max} value at 4.5 mg/g. The H500 biochar has the second highest q_{max} value at 2.56 mg of copper bound per gram of biochar and the third highest *K* value for affinity for copper. Both the H500 and H700 are the most promising out of all of the biochars due to their high q_{max} and relatively high *K* values. Both of these biochars have higher q_{max} values compared to the GAC but have lower *K* values. Figures 4.9 and 4.10 below show the experimental data, Langmuir model, and Freundlich model (both using the calculated constants) for the H500 and H700 biochars respectively.

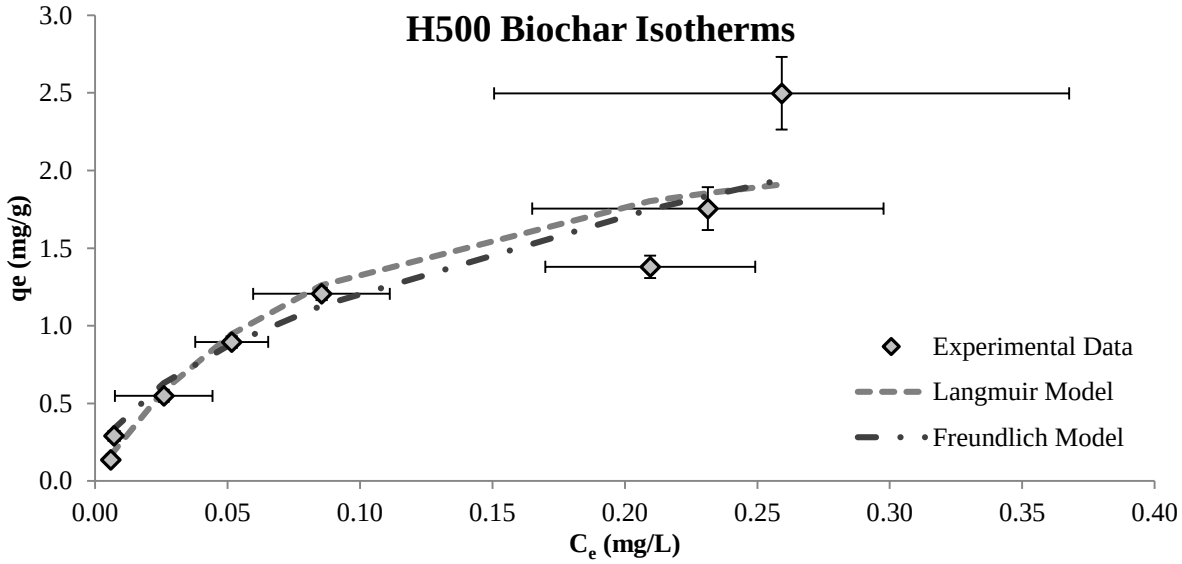

Figure 4.9- Experimental data and Freundlich and Langmuir fitted isotherm models for H500.

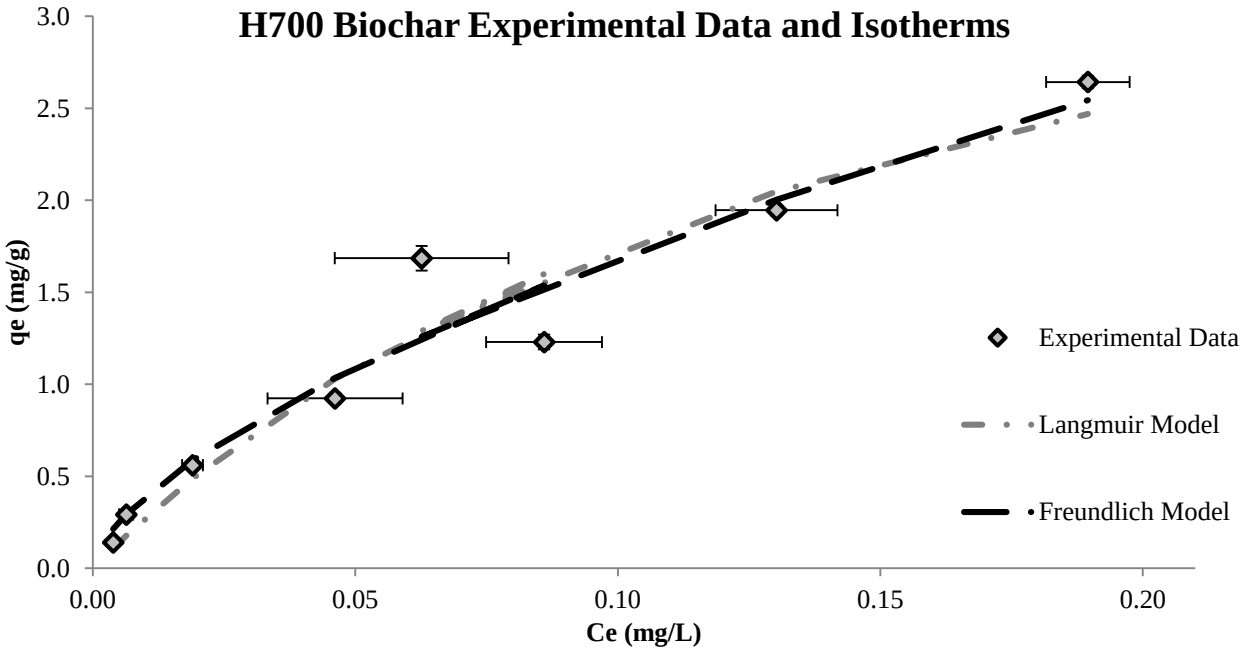

Figure 4.10- The experimental data, Langmuir, and Freundlich models are shown for the H700 biochar. The Freundlich and Langmuir model equations are shown next to the legend icon for that isotherm.

Figures 4.11 and 4.12 below show the experimental data for the hazelnut shell and Douglas fir chars respectively. The steeper slope for the H700 and H500 data indicates that those biochars have significantly better copper adsorption than the H300.

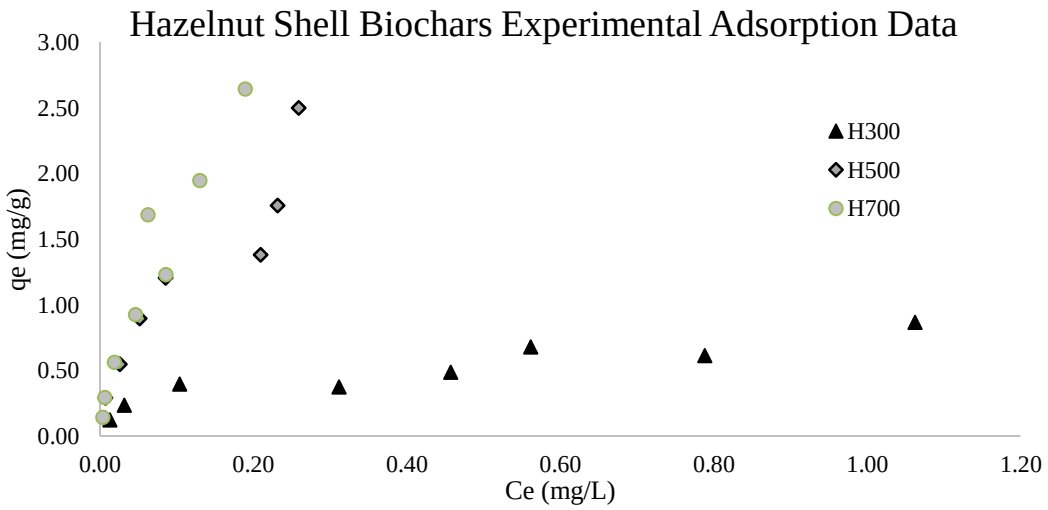

Figure 4.11- Experimental isotherm data for hazelnut shell chars (H700, H500, and H300).

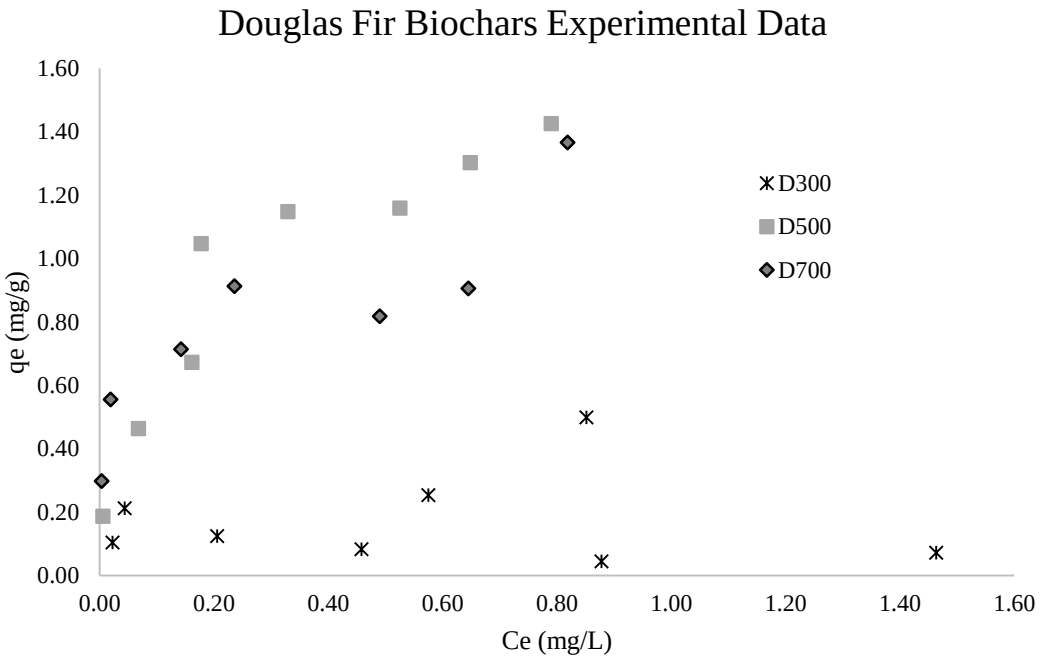

Figure 4.12- Experimental isotherm data for Douglas fir wood chips chars (D700, D500, and D300).

At initial copper concentrations closest to those measured in stormwater (between 9.08 µg/L and 40.9 µg/L) the H700, H500, and D700 biochars performed the best according to percent copper removed from aqueous phase during the 48 hour run time for the batch isotherm experiments. Table 4.2 shows the percent of copper removed by each biochar at an initial aqueous copper concentration of 75 ppb.

Table 4.2-The percent of copper removed from the solution after 48 hours into the batch test (once equilibrium has been reached).

	Percent Copper Removed					
Initial Copper Concentration (ppb)	**D300**	**D500**	**D700**	**H300**	**H500**	**H700**
75	69.9	71.2	96.9	82.9	92.1	94.8

GAC was not tested for an initial copper concentration of 75 ppb but had an average removal of 89.8% for an initial copper concentration of 100 ppb. So the H700, H500, and D700 biochars are all on par with the GAC in terms of copper adsorption. Based on the modeling parameters for both Langmuir and Freundlich models as well as the

percentage removal of copper from solution by the biochar, the H700 and H500 biochars can be concluded to work the best for copper removal out of the six biochars studied. Overall trends for the biochars show that, in general, the hazelnut shell feedstock biochars are more effective at adsorbing copper from the synthetic stormwater solution than the Douglas fir biochars. Additionally, the effectiveness of the biochars increases with increasing pyrolysis temperature which is by both the percent copper removed from aqueous phase in Table 4.2 and in both Figures 4.11 and 4.12.

Figure 4.13 shows a comparison between the performance of H700, H500, D700, and GAC for copper adsorption.

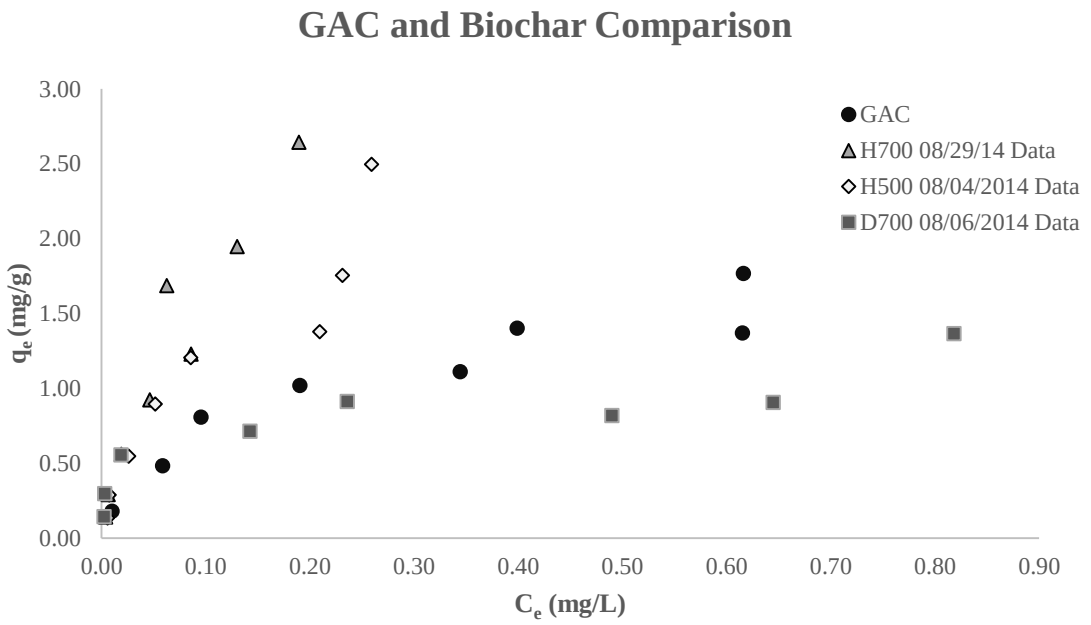

Figure 4.13- GAC compared to the H700, H500, and D700 biochars for copper adsorption.

Both the H700 and H500 chars perform better than the GAC at all copper concentrations tested. The D700 adsorbs copper better at low concentrations (the range found in stormwater runoff) than the GAC but does not work as well at higher copper concentrations.

Additional isotherm experiments were run on the D300, D700, H500, and H700 chars at the higher end of the range of initial copper concentrations (700-1500 ppb) than were originally run. This was prompted by high variation in the standard deviation in the equilibrium concentrations measured for the higher range initial concentrations. The entire D300 concentration range was re-tested instead of just the higher concentration range due to the multiple outliers and a negative value calculated for q_e. For all of the biochars, the data collected in the second round of isotherm testing showed much more copper adsorbed onto the biochar (higher q_e value) than for those same initial concentration ranges in the first round of testing on those chars. Figure 4.14 below shows a comparison of the data for the initial batch isotherm tests conducted in 2014 and the data obtained from the second batch tests conducted in 2015.

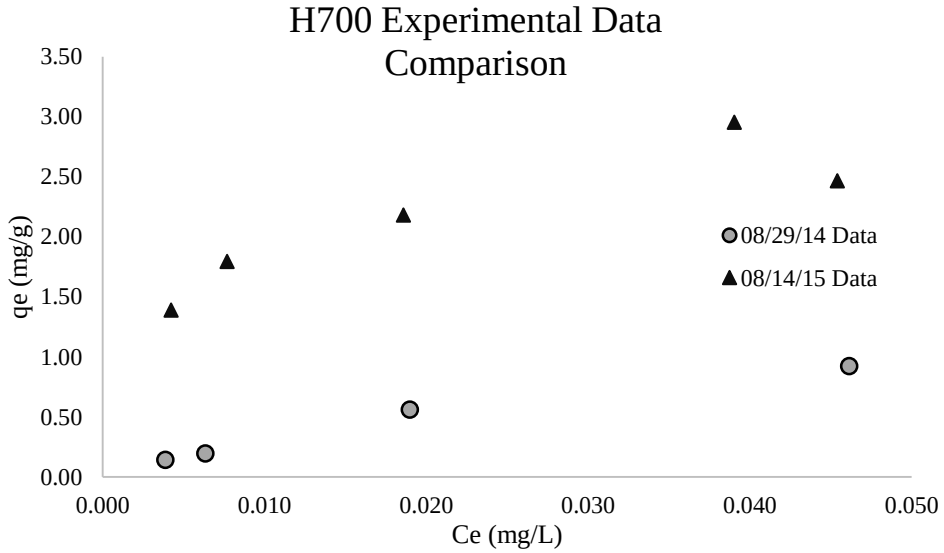

Figure 4.14-Comparison for H700 biochars copper adsorption data for 700-1500 ppb initial copper concentration range.

Time did not permit further investigation into possible causes for this increase in copper adsorption. All of the data obtanied from this second round of isotherm testing can be found in the Appendix.

4.1.3. Synthetic Stormwater with SRNOM Batch Isotherm Test Results

Additional batch isotherm tests were run on the H700 and H500 biochar with Suwanee River Natural Organic Matter (SRNOM) added to more accurately replicate the NOM that would be present in the stormwater. The data was analyzed using the same methods as described above. Table 4.3 below shows a comparison of R^2 values, Freundlich, and Langmuir constants between the H500 and H700 biochars with SRNOM included in the synthetic stormwater solution and the H500 and H700 biochars without SRNOM.

Table 4.3-Comparison of isotherm constants and SSE values for H500 and H700 biochars with SRNOM and the H500 and H700 biochars without SRNOM.

SRNOM Isotherm Parameters Comparison			
Langmuir			
Biochar	q_{max} **(mg/g)**	K **(L/mg)**	***SSE***
H500	2.56	11.35	2.81
H700	4.50	6.42	1.55
H500 SRNOM	8.31	0.33	0.28
H700 SRNOM	0.00	0.00	30.51
Freundlich			
Biochar	***n***	K_f	***SSE***
H500	2.05	3.75	2.96
H700	1.57	7.34	1.31
H500 SRNOM	1.1	2.21	0.31
H700 SRNOM	1.98	1.92	10.34

As expected based on the earlier batch tests conducted without SRNOM, the H500 and H700 biochars still have slightly lower *SSE* values overall value for the Freundlich isotherm model than for the Langmuir model. In the Langmuir model,

while the H500 test conducted with SRNOM has a higher q_{max} value than the H500 test conducted without SRNOM, the *SSE* value is so high that the calculated constants for model are not very useful. Additionally, for the H700 test with SRNOM the q_{max} and *K* values were calculated as zero due to the Langmuir model fitting the data so poorly. No conclusions can be drawn for the Langmuir model of the H700 biochars with SRNOM, except that this model does not accurately describe the adsorption process that occurred during this test.

Both of the biochars tested with NOM have *1/n* values that are less than one so it is still favorable for the copper to sorb onto those biochars even in the presence of SRNOM. In a comparison between the H500 char with and without NOM, the *n* value decreased when NOM was added, making it less favorable for copper to sorb to the biochar in the presence of NOM than without it. However, for the H700 biochar, the *n* value increased with the addition of SRNOM to the test. Additionally, the K_f value decreased for both biochars for the tests where NOM was added.

Figures 4.14 and 4.15 below show the differences between both of the biochars with and without SRNOM. The Freundlich isotherm model is used to represent this data since is the *SSE* value shows it to be more accurate to describe the range of initial copper concentrations that were tested compared to the Langmuir isotherm model.

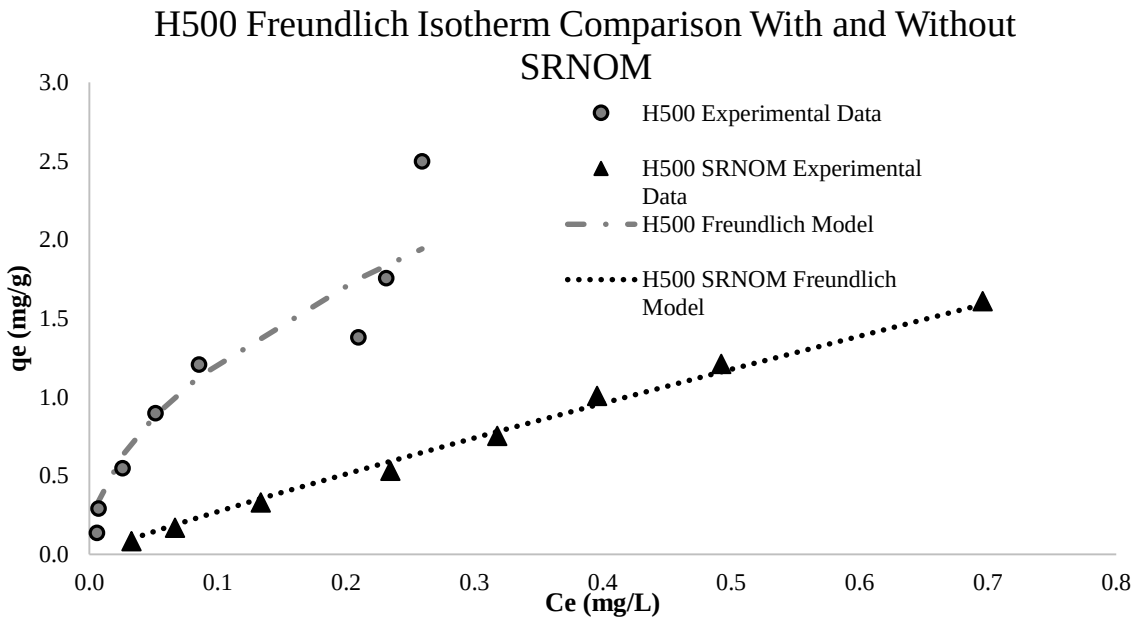

Figure 4.15-This shows a comparison of the experimental data gathered for the H500 biochar batch isotherm tested with and without SRNOM. The dashed lines on the graph represent Freundlich isotherm models created using the equilibrium aqueous concentrations of copper for each test and the Freundlich constants displayed in Table 4.3.

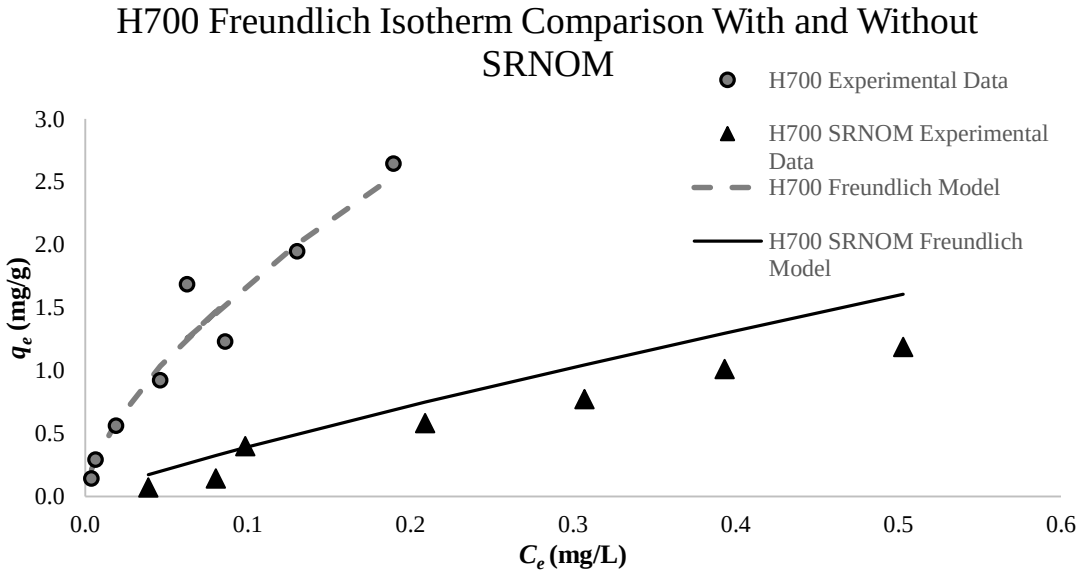

Figure 4.16-This shows a comparison of the experimental data gathered for the H700 biochar batch isotherm tested with and without SRNOM. The dashed lines on the graph represent Freundlich isotherm models created using the equilibrium aqueous concentrations of copper for each test and the Freundlich constants displayed in Table 4.3.

Since the *n* values for both the H500 and H700 SRNOM tests are closer to one compared to the versions of the test without SRNOM, the Freundlich model for the SRNOM tests is closer to linear. The lower adsorption observed when SRNOM is added to the stormwater was expected based off currently published literature in that adding NOM to batch isotherm tests causes less copper to be adsorbed by the biochars. This could potentially be due to competition between copper and the NOM for adsorption sites but is more likely caused by complexation of copper with the NOM which prevents it from being adsorbed by the biochar. This is not beneficial as in real world scenarios the copper that had complexed with the NOM would pass through the biochar media filter and continue into a nearby waterbody. The copper has the potential to separate from the NOM and once again be dissolved in the water where it can affect salmon's olfactory senses.

4.2. Biochar Characterization

Multiple tests were conducted to characterize the biochars to find out which properties of the biochars were linked to higher copper adsorption from the stormwater solution. These tests included measuring the surface area and pH of the biochar, and performing thermogravimetric analysis (TGA), proximate carbon analysis, and Fourier-transform infrared spectroscopy (FTIR).

4.2.1. Thermogravimetric Analysis

The thermogravimetric analysis (TGA) was performed on the two initial feedstocks (hazelnut shells and Douglas fir wood chips), not the biochars created from them. This experiment, in addition to the proximate carbon analysis and FTIR experiments discussed later, provides valuable insight into how much and what parts of the

feedstock are lost at different pyrolysis temperatures. Figure 4.17 below shows the change in weight remaining for each of the feedstocks as the temperature increases.

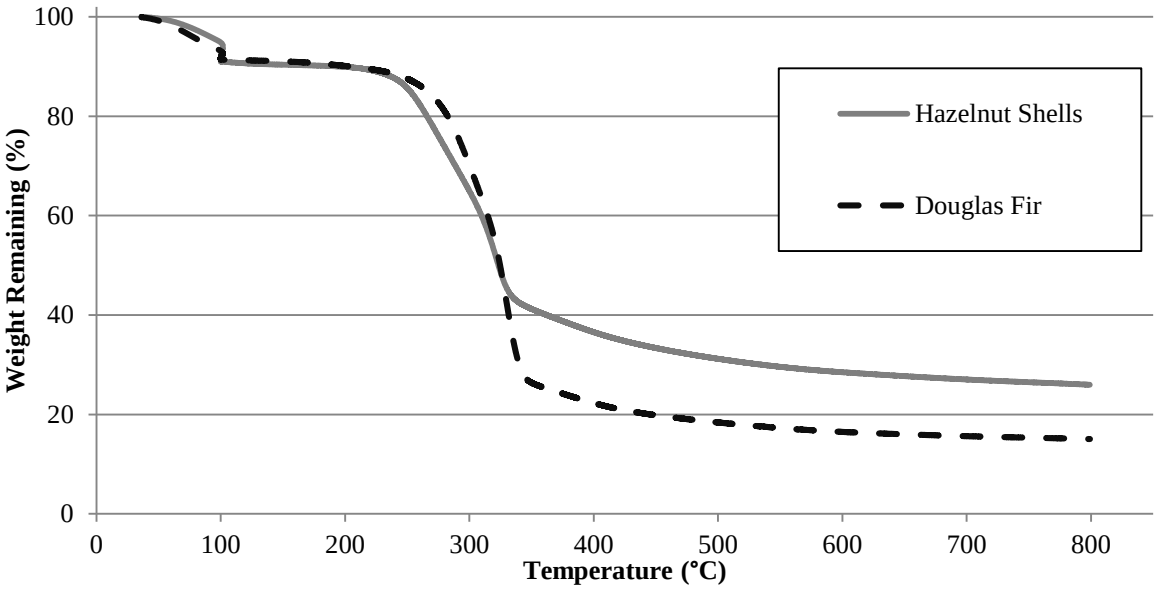

Figure 4.17- This graph shows the decrease in feedstock mass as temperature increases over time.

Table 4.4 below shows the measured percent weight remaining at the pyrolysis temperatures that were used to create the biochars to give an estimate of how much of the feedstock is lost at those temperatures.

Table 4.4-Measured percent weight remaining for both feedstocks at the biochar pyrolysis temperatures.

	Percent Weight Remaining (%)	
TGA Temperature	**Hazelnut Shell Feedstock**	**Douglas Fir Feedstock**
300°C	64.95	70.14
500°C	31.19	18.4
700°C	27.03	15.64

Most of the mass of the feedstocks were volatilized between 250 and 350°C. While both feedstocks lose mass at about the same rate and during the same time period, the hazelnut shells plateau sooner that the Douglas fir feedstock, resulting in a higher percent remaining for the hazelnut compared to the Douglas fir. Since the weight

percent change levels off faster in hazelnut shells, it can be assumed that they have less volatile matter in the feedstock (which generally is volatilized from around 250-400°C) and larger ash content than the Douglas fir feedstock does.

4.2.2. Proximate Carbon Analysis

All of the six biochars and commercially available Calgon granular activated carbon (GAC) were tested in this experiment. Figure 4.18 below shows all of the biochars and the GAC broken down into percentages of volatile matter, fixed carbon, and ash. Both the hazelnut shell and Douglas fir biochars have increasing fixed carbon content and decreasing volatile matter content as the pyrolysis temperatures increase. For each pyrolysis temperature char, the hazelnut chars had higher fixed carbon content and lower volatile matter content compared to the Douglas fir chars pyrolyzed at the same temperature.

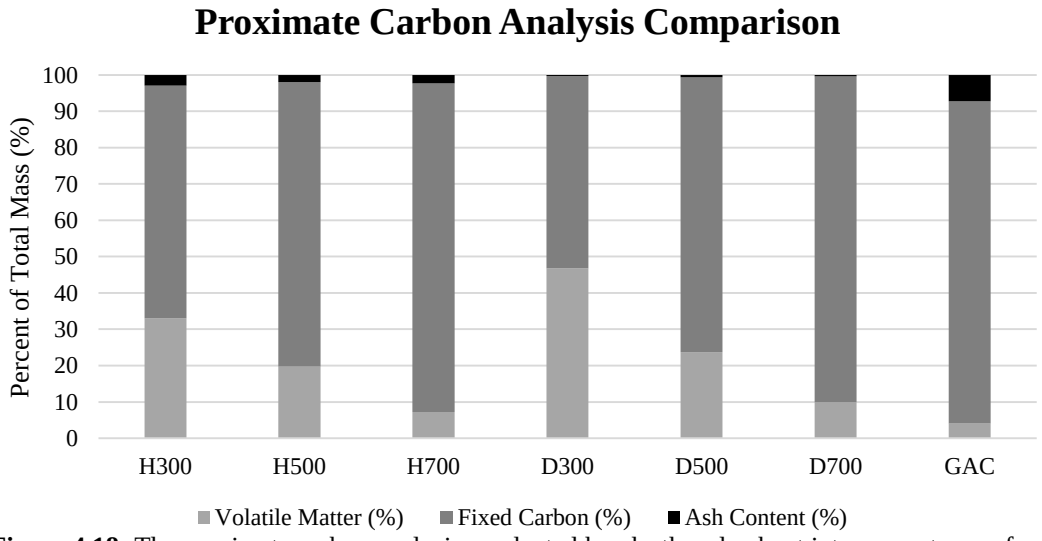

Figure 4.18- The proximate carbon analysis conducted breaks the adsorbent into percentages of volatile matter, fixed carbon, and ash content. The volatile matter portion of the adsorbent burns off first, then the fixed carbon, and all that remains at the end is the ash content.

Additionally, while the hazelnut chars and GAC both have an ash content of around 2% or higher, the Douglas fir biochars have less than 1% ash content in any of those chars. Ash content does not appear to be largely affected by the pyrolysis temperature

of the biochar for either the hazelnut shells or Douglas fir biochars. The hazelnut shell biochar ash content ranges from 1.97%-2.9% and the Douglas fir biochar has a range of 0.3%-0.66% as seen below in Table 4.5.

Table 4.5- Each of the biochars and the GAC are broken down into their percentage composition of volatile matter, fixed carbon, and ash content.

Adsorbent	Volatile Matter (%)	Fixed Carbon (%)	Ash Content (%)
H300	33.00	64.10	2.90
H500	19.78	78.25	1.97
H700	7.19	90.52	2.29
D300	46.80	52.90	0.30
D500	23.74	75.61	0.66
D700	9.96	89.68	0.36
GAC	4.10	88.60	7.30

By comparing the results from this experiment with the batch isotherm results, it can be concluded that increased fixed carbon content in the biochars is correlated to increased copper adsorption. This is not true for the GAC as it has much higher fixed carbon composition but does not adsorb copper as well as the higher pyrolysis temperature biochars. Additionally, it has a much higher ash content than any of the biochars tested.

4.2.3. Biochar pH Test Results

Since there were duplicate samples for each of the biochars, the average between the two final pHs at the end of the experiment was taken and those are displayed in Table 4.6 below. The full data set with the individual measurements for each of the duplicate samples can be found in the Appendix. The pH of the 0.01 M $CaCl_2$ solution that the biochars were suspended in was determined to be 5.44 initially before any biochars were put into the solution.

Table 4.6-Average pH measured at the end of the 24 hours in the tumbler for each of the six biochars.

Sample	Average pH	Standard Deviation
D300	4.37	0.014
D500	6.615	0.205
D700	7.605	0.233
H300	8.075	0.007
H500	9.545	0.007
H700	8.505	0.035

Overall, there is a trend that as the pyrolysis temperature increases, so does the measured pH for the biochar. This can likely be attributed to more organic acids being volatilized from the biochars as the pyrolysis temperature increases, which is also hinted at by the TGA data discussed previously. The only exception to this trend is that the H500 biochar's pH is significantly higher that the H700 biochar's pH. Surprisingly, the D300 biochar has a lower measured pH than the pH of the 0.01 M $CaCl_2$ solution. Additionally, all of the hazelnut shell biochars have higher pH measurements than the Douglas fir produced at equal temperature. Based on this data, it can be concluded that there is a correlation between higher biochar pH and increased copper adsorption. This matches the literature precedent of increased adsorption in solutions with pH between 5 and 10 as discussed in the literature review.

4.2.4. Biochar BET Surface Area Results

Table 4.7 and Figure 4.19 display the measured BET surface area for all six of the biochars.

Table 4.7-Surface area determined using the BET method for all six biochars.

Biochar	BET Surface Area
D300	3.8784 m^2/g
D500	325.7194 m^2/g
D700	597.1453 m^2/g
H300	0.5449 m^2/g
H500	73.8459 m^2/g
H700	423.3706 m^2/g
GAC	1730.7639 m^2/g

A trend seen in both the hazelnut shells and Douglas fir biochars is that as pyrolysis temperature increases, so does the surface area of the biochar. However, the biochars made from Douglas fir wood chips have higher surface areas at each pyrolysis temperature compared to the respective hazelnut shells biochar made at those same temperatures. This is likely due to the wood chips being a more porous feedstock than the hazelnut shells and this property carried over to the biochar when the feedstock was pyrolyzed. Interestingly, the GAC has much higher surface area than any of the biochars tested but does not perform as well as the H700, D700, and H500.

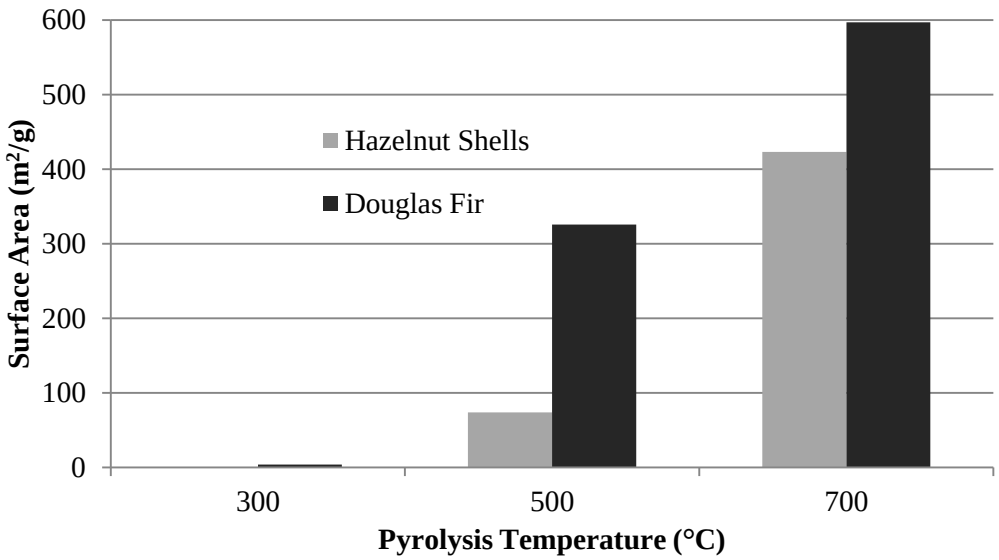

Figure 4.19-BET surface area recorded for each biochar

Although higher surface area is generally correlated to better copper adsorption in biochars, the higher surface areas for the Douglas fir compared to the hazelnut shells chars did not result in better copper adsorption by the Douglas fir biochars than the hazelnut biochars across the same pyrolysis temperature.

4.2.5. Functional Group Analysis-Fourier Transform Infrared Spectroscopy

As expected from literature, the number of functional groups measured decreases with increasing pyrolysis temperature. The functional groups found by the IR Spectral Interpretation database based off of the IR peaks measured for the Douglas fir biochars are displayed in Table 4.8 below. The D700 biochar is not included in Table 4.8 as the database could not find any matches for the peaks displayed.

Table 4.8- IR peaks measured for D300 and D500 biochars. * denotes the source as (Coates 2000), while ** refers to an EPA document assigning characteristic vibrations to individual peaks in wood and grass char ATR FT-IT spectra. '- ' denotes that a specific functional group determined by the IR Spectral database was not able to be confirmed using the other two literature sources specificed above.

Douglas Fir Biochar IR Spectra Peaks				
IR Spectral Analysis Database		**Literature Functional Group Analysis**		
Experimental Peak Wavenumber Range (cm^{-1})	**Database Compound Groups**	**Literature Wavenumber range (cm^{-1})**	**Characteristic Vibrations**	**Functionality**
D300 Biochar Peaks				
1180-1265	Phenols	~1200	C-O stretch	Phenol*
3250-3600		3530-3640	O-H stretch	Phenol*
1220-1270	Aromatic Ethers	1230-1270	C-O stretch	C-O-C groups and aryl ethers**
1590-1630	Aliphatic Amino Acids	1580-1615	Aromatic ring stretch	Aromatic amino acid*
2500-3200		~2885, ~2935, ~3050, ~3200	C-H stretch	likely aliphatic CH_x**
1340-1380	Aliphatic Hydrocarbons	1330-1350	Methyne C-H bend	Saturated aliphatic group*
1440-1480		1445-1485	Methylene C-H bend	Saturated aliphatic group*
2830-2970		2860-2880, 2845-2865, 2915-2935, 2950-2970	C-H asym/sym stretch (Methyl or Methylene)	Saturated aliphatic group*
D500 Biochar Peaks				
~1400	Aliphatic Amino Acids	~1440	C=C stretch	aromatic C, indicative of lignin, appears when bound to unsaturated group**
~1500		~1510	C=C stretch	aromatic skeletal vibrations, indicative of lignin**
~1600		~1600	C=C stretch	aromatic components**
2840-2970		2860-2880, 2845-2865, 2915-2935, 2950-2970	C-H asym/sym stretch (Methyl or Methylene)	Saturated aliphatic group*
980	Inorganic Sulfates	-	-	-
1050-1200		1080-1130	-	Sulfate ion*
3300-3600		-	-	-

Figure 4.20 below shows a plot of the IR spectra measured for the Douglas fir biochars.

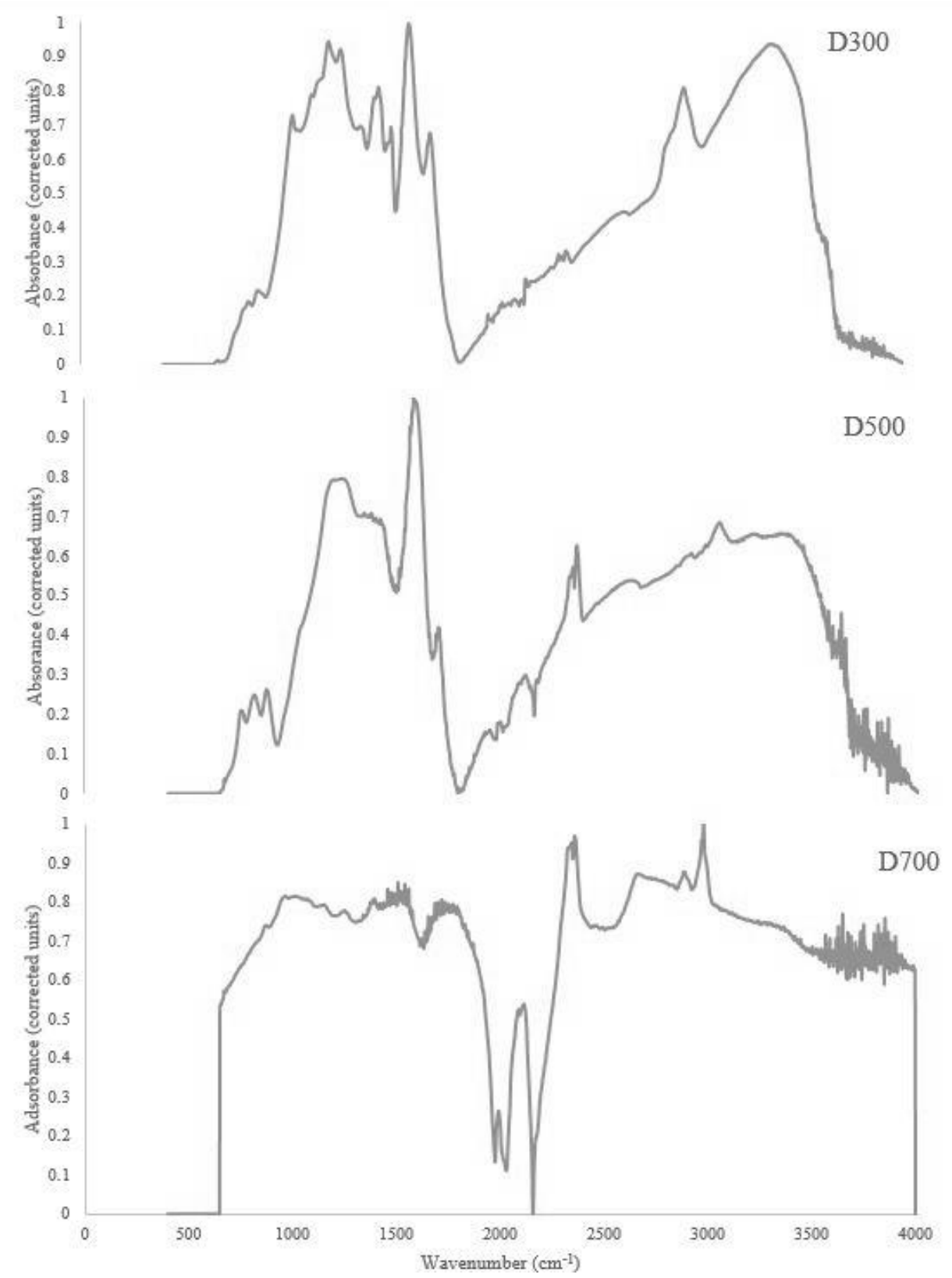

Figure 4.20- FTIR data for D300, D500, and D700 biochars.

The phenols and ethers that are present in the D300 biochar are not present in D500 biochar, likely due to the volatilization between 250-350°C as discussed regarding the TGA feedstock data. The aliphatic amino acids were present in both the D300 and D500 biochars. For the D500 char, there were additional IR peaks at the wavenumbers which correspond to inorganic sulfates, which were not present in the D300 char. The broad peak located between 2150-4000 cm^{-1} increases in size as the pyrolysis temperature increases. The sharp peak around 1700 cm^{-1} that is present for both the D300 and D500 chars does not occur in the D700 char.

The functional groups determined for the hazelnut biochars based on characteristic wavenumber ranges found in literature are shown in Tables 4.9 and 4.10 below.

Table 4.9- IR peaks measured for H300 and H500 biochars.

Hazelnut Shell Biochar IR Spectra Peaks				
IR Spectral Analysis Database		**Literature Functional Group Analysis**		
Experimental Peak Wavenumber Range (cm^{-1})	**Database Compound Groups**	**Literature Wavenumber range (cm^{-1})**	**Characteristic Vibrations**	**Functionality**
H300 Biochar Peaks				
780-870	Aliphatic Primary Amines	~750, ~815, ~885	C-H bending	aromatic CH out-of-plane deformation**
1070-1095		1020-1090	C-N stretch	primary amine*
1570-1630		1590-1650	N-H bend	primary amine*
3270-3295		-	-	-
3310-3330		3325-3345	N-H stretch	Aliphatic primary amine*
~750	Aliphatic Hydrocarbon	~750	C-H bending	aromatic CH out-of-plane deformation**
~1380		1380-1385	*gem*-Dimethyl or "iso"-doublet	Saturated aliphatic methyl group*
~1460		1445-1485	Methylene C-H bend	Saturated aliphatic group*
2840-2960		2860-2880, 2845-2865, 2915-2935, 2950-2970	C-H asym/sym stretch (Methyl or Methylene)	Saturated aliphatic group*
H500 Biochar Peaks				
~700	Inorganic carbonate	-	-	-
~900		860-880	-	Carbonate ion*
1300-1500		1410-1490	-	Carbonate ion*
~2500		-	-	-
3200-3560		3200-3500	O-H stretch	H-bonded hydroxyl groups**
1400-1450	Aliphatic Carboxylic Acid Salts	1300-1420	-	Carboxylate*
1560-1580		1550-1610	-	Carboxylate*
~750	Aliphatic Hydrocarbons	~750	C-H bending	aromatic CH out-of-plane deformation**
~1360		1365-1370	*gem*-Dimethyl or "iso"-doublet	Saturated aliphatic methyl group*
~1450		1445-1485	Methylene C-H bend	Saturated aliphatic group*
2850-2950		2860-2880, 2845-2865, 2915-2935, 2950-2970	C-H asym/sym stretch (Methyl or Methylene)	Saturated aliphatic group*

Table 4.10- IR peaks measured for H700 biochar.

Hazelnut Shell Biochar IR Spectra Peaks				
IR Spectral Analysis Database		**Literature Functional Group Analysis**		
Experimental Peak Wavenumber Range (cm^{-1})	**Database Compound Groups**	**Literature Wavenumber range (cm^{-1})**	**Characteristic Vibrations**	**Functionality**
H700 Biochar Peaks				
~750	Aliphatic Hydrocarbon	~750	C-H bending	aromatic CH out-of-plane deformation**
~1360		1365-1370	*gem*-Dimethyl or "iso"-doublet	Saturated aliphatic methyl group*
~1450		1445-1485	Methylene C-H bend	Saturated aliphatic group*
2850-2950		2860-2880, 2845-2865, 2915-2935, 2950-2970	C-H asym/sym stretch (Methyl or Methylene)	Saturated aliphatic group*

Aliphatic hydrocarbons are present for all three different pyrolysis temperature hazelnut biochars and are the only functional group in the H700 char. This group may be linked to the increased copper adsorption compared to the Douglas fir chars at each temperature. The H500 char has inorganic carbonate groups which are not present in either the lower temperature H300 char or the higher temperature H700 char. This mirrors what is seen for the D500 biochar but is inorganic carbonate instead of inorganic sulfates. These are potentially left behind as part of the biochar when the majority of the volatiles are burnt off around 300-400°C but cannot withstand the temperatures above 500°C so they volatilize before 700°C, which would be why inorganic carbonates are not present in the H700 or H300 but are in the H500.

Figure 4.21 below shows the FTIR spectra for the hazelnut shell biochars.

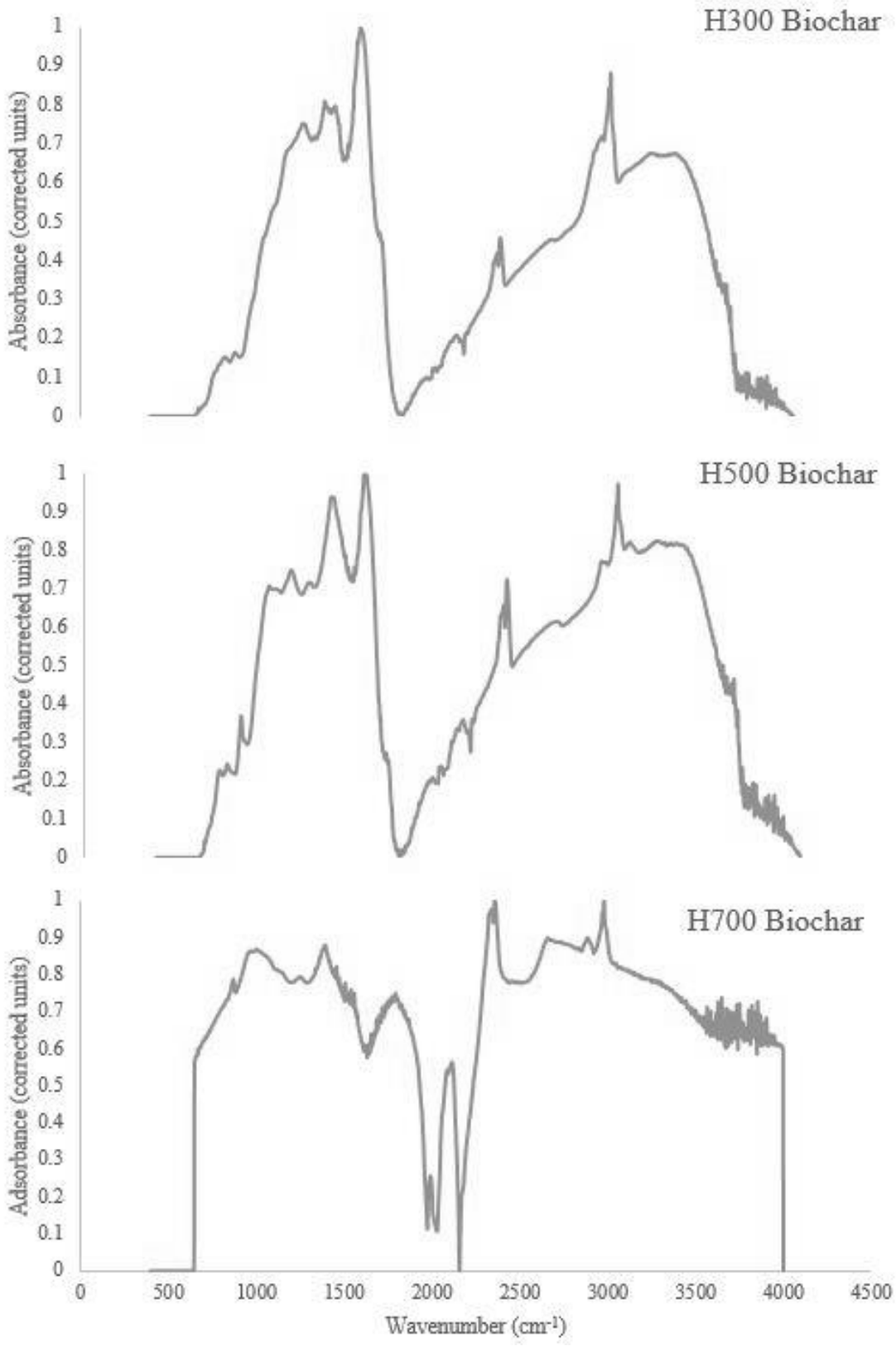

Figure 4.21- FTIR data for H300, H500, and H700 biochars.

5. CONCLUSION

The primary objective of this research wasto determine which biochar properties were correlated to increased copper adsorption by those chars in hopes that this could allow for the creation of more effective biochars and a better understanding of the adsorption mechanism of copper onto biochar. This was accomplished by conducting batch isotherm adsorption experiements and characterization on the six biochars used as part of this research. The major findings of this study are:

1. Increased pyrolysis temperature correlates to increased copper adsorption by the biochar. When compared for each pyrolysis temperature, the hazelnut shell based biochars performed better than the Douglas fir based biochars. However, at the copper concentrations that would be present in stormwater, the D700, H500, and H700 biochars perform the best out of the six biochars. Overall, the chars pyrolyzed in the range of 500-700°C correlated to the highest copper adsorption. As far as implications for practical applications of this work, since the lower pyrolysis temperature H500 char has almost equal effectiveness to the higher temperature H700 char, the H500 may acutally be the more optimal biochar in terms of cost effectiveness. The H500 char requires less energy to produce since it has a lower pyrolysis temperature than the H700 char and therefore could be more cost effective for large scale applications.
2. The Douglas fir biochars are modeled best by the Langmuir isotherm while the hazelnut shell biochars are modeled best by the Freundlich isotherm based on the initial copper concentration rages tested. However,higher initial

concentration ranges are needed to verify these findings as none of the experimental data isotherms have reached the plateau associated with those models.

3. Increased copper adsorption onto biochar can be linked to high biochar pH, higher fixed carbon percentage (and therefore decreased volatile matter percentage), and higher surface area. Having a high surface area is not likely the determining factor for what makes biochar adsorb copper more effectively as the Douglas fir biochars had higher surface areas than the hazelnut chars at each of the pyrolysis temperatures but overall had lower copper adsorption.
4. Ash content does not drastically change as a function of pyrolysis temperature but instead appears to be a property of the intial feedstock that remains fairly constant over all of the pyrolysis temperatures.
5. Based on the FTIR spectra for the chars, inorganic functional groups appear on the 500°C chars but not on any of the other temperature biochars. Additionally, for the hazelnut chars, the aliphatic hydrocarbons are the only overall functional group that is present for all three temperatures. The functional groups that correspond to those IR peaks could potentially be responsible for some of the increased copper adsorption.

Overall, it was concluded that higher pyrolysis temperature is correlated to higher surface area, greater loss of volatiles, and higher pH (from volatilizatin of organic acids). In turn, all of the above mentioned characteristics are correlated to increased copper adsorption. Lastly, based on the isotherm results, it appears that the higher

temperature range biochars prove better at copper adsorption compared to the GAC even without the steam activation step.

5.1. Future Work

There are still some unanswered questions about the second set of batch isotherms that were run that had dramatically higher copper adosrbance over the same initial copper concentration. While it is unlikely that the biochar's surface area changed in the year between the two sets of batch tests, if any microbial activity or oxidation of the biochars, those could potentially alter the biochar's ability to adsorb copper. Comparison pH, proximate carbon analysis, and FTIR could show any changes that might have occurred in that year long span. Additionally, other experimental characterization procedures that were also mentioned in many of the literatures sources cited such as zeta potential, CHNO analysis, continuous flow tests (media filter), and adsorption isotherms generated using collected stormwater.

6. LITERATURE CITED

AMEI. "Thermogravimetry (TG) or Thermogravimetric Analysis (TGA) or Thermal Gravimetric Analysis." Anderson Materials Evaluation Inc. Web. 17 Mar. 2016.

Armagan, Bulent, and Fatih Toprak. "Optimum Isotherm Parameters for Reactive Azo Dye onto Pistachio Nut Shells: Comparison of Linear and Non-Linear Methods." Polish Journal of Environmental Studies 22.4 (2013): 1007-011. Web.

Baldwin, David H., Christopher P. Tatara, and Nathaniel L. Scholz. "Copper-induced Olfactory Toxicity in Salmon and Steelhead: Extrapolation across Species and Rearing Environments." Aquatic Toxicology 101.1 (2011): 295-97. Web.

Biniak, S., M. Pakuła, G. S. Szymański, and A. Świątkowski. "Effect of Activated Carbon Surface Oxygen- And/or Nitrogen-Containing Groups on Adsorption of Copper (II) Ions from Aqueous Solution." Langmuir 15.18 (1999): 6117-122. Web.

Brewer, Catherine Elizabeth. Biochar Characterization and Engineering. Thesis. Digital Repository at Iowa State University, 2012. Print.

Chen, Xincai, Guangcun Chen, Linggui Chen, Yingxu Chen, Johannes Lehmann, Murray B. Mcbride, and Anthony G. Hay. "Adsorption of Copper and Zinc by Biochars Produced from Pyrolysis of Hardwood and Corn Straw in Aqueous Solution." Bioresource Technology 102.19 (2011): 8877-884. Web.

Coates, John. "Interpretation of Infrared Spectra, A Practical Approach." Encyclopedia of Analytical Chemistry. 2000. Print.

State of Washington Department of Ecology. "Better Brakes Law." Hazardous Waste & Toxics Reduction. State of Washington Department of Ecology. Web. 15 Mar. 2016.

Desta, Mulu Berhe. "Batch Sorption Experiments: Langmuir and Freundlich Isotherm Studies for the Adsorption of Textile Metal Ions onto Teff Straw (Eragrostis Tef) Agricultural Waste." Journal of Thermodynamics 2013 (2013): 1-6. Web.

EPA (2016a) "Granular Activated Carbon." Drinking Water Treatability Database. Environmental Protection Agency. Web. 10 Mar. 2016.

EPA (2016b) "GAC Isotherm." Drinking Water Treatability Database. Environmental Protection Agency. Web. 10 May 2016.

EPA (2016c) "Secondary Drinking Water Standards: Guidance for Nuisance Chemicals." EPA. Environmental Protection Agency. Web. 10 Mar. 2016.

Ho, Yuh-Shan, Wen-Ta Chiu, and Chung-Chi Wang. "Regression Analysis for the Sorption Isotherms of Basic Dyes on Sugarcane Dust." Bioresource Technology 96.11 (2005): 1285-291. Web.

Huggins, Tyler, Heming Wang, Joshua Kearns, Peter Jenkins, and Zhiyong Jason Ren. "Biochar as a Sustainable Electrode Material for Electricity Production in Microbial Fuel Cells." Bioresource Technology 157 (2014): 114-19. Web.

IBI (2016a) "Biochar Production Units." International Biochar Initiative. Web. 12 Mar. 2016

IBI (2016b) "Profile: Three Dimensional Timberlands – Sustainable Biomass Pyrolysis Using Forestry Waste." International Biochar Initiative. Web. 12 Mar. 2016.

Kayhanian, M., C. Suverkropp, A. Ruby, and K. Tsay. "Characterization and Prediction of Highway Runoff Constituent Event Mean Concentration." Journal of Environmental Management 85.2 (2007): 279-95. Web.

Keiluweit, Marco, Peter S. Nico, Mark G. Johnson, and Markus Kleber. "Dynamic Molecular Structure of Plant Biomass-Derived Black Carbon (Biochar)." Environmental Science & Technology Environ. Sci. Technol. 44.4 (2010): 1247-253. Web.

Kim, Kwang Ho, Jae-Young Kim, Tae-Su Cho, and Joon Weon Choi. "Influence of Pyrolysis Temperature on Physicochemical Properties of Biochar Obtained from the Fast Pyrolysis of Pitch Pine (Pinus Rigida)." Bioresource Technology 118 (2012): 158-62. Web.

Manyà, Joan J. "Pyrolysis for Biochar Purposes: A Review to Establish Current Knowledge Gaps and Research Needs." Environmental Science & Technology Environ. Sci. Technol. 46.15 (2012): 7939-954. Web.

Mcbeath, Anna V., Christopher M. Wurster, and Michael I. Bird. "Influence of Feedstock Properties and Pyrolysis Conditions on Biochar Carbon Stability as Determined by Hydrogen Pyrolysis." Biomass and Bioenergy 73 (2015): 155-73. Web.

Mcintyre, Jenifer K., David H. Baldwin, David A. Beauchamp, and Nathaniel L. Scholz. "Low-level Copper Exposures Increase Visibility and Vulnerability of Juvenile Coho Salmon to Cutthroat Trout Predators." Ecological Applications 22.5 (2012): 1460-471. Web.

Mohan, Dinesh, and Charles U. Pittman, Jr. "Activated Carbons and Low Cost Adsorbents for Remediation of Tri- and Hexavalent Chromium from Water." Journal of Hazardous Materials 137.2 (2006): 762-811. Web.

Mohan, Dinesh, and Charles U. Pittman. "Arsenic Removal from Water/wastewater Using Adsorbents—A Critical Review." Journal of Hazardous Materials 142.1-2 (2007): 1-53. Web.

Morace, Jennifer L. "Water-Quality Data, Columbia River Estuary, 2004-05." Water-Quality Data, Columbia River Estuary, 2004-05. USGS. Web. 10 Mar. 2016.

Mukherjee, A., A.r. Zimmerman, and W. Harris. "Surface Chemistry Variations among a Series of Laboratory-produced Biochars." Geoderma 163.3-4 (2011): 247-55. Web.

Nason, Jeffrey A., Don J. Bloomquist, and Matthew S. Sprick. "Factors Influencing Dissolved Copper Concentrations in Oregon Highway Storm Water Runoff." J. Environ. Eng. Journal of Environmental Engineering 138.7 (2012): 734-42. Web.

Ncibi, Mohamed Chaker. "Applicability of Some Statistical Tools to Predict Optimum Adsorption Isotherm after Linear and Non-linear Regression Analysis." Journal of Hazardous Materials 153.1-2 (2008): 207-12. Web.

NMFS. "5-Year Review: Summary and Evaluation of Upper Willamette River Steelhead and Upper Willamette River Chinook." National Marine Fisheries Service, 26 July 2011. Web. 10 Mar. 2016.

Osmari, Taynara, Roger Gallon, Marcio Schwaab, Elisa Barbosa-Coutinho, João Severo, and José Pinto. "Statistical Analysis of Linear and Non-linear Regression for the Estimation of Adsorption Isotherm Parameters." Adsorption Science & Technology 31.5 (2013): 433-58. Web.

Regmi, Pusker, Jose Luis Garcia Moscoso, Sandeep Kumar, Xiaoyan Cao, Jingdong Mao, and Gary Schafran. "Removal of Copper and Cadmium from Aqueous Solution Using Switchgrass Biochar Produced via Hydrothermal Carbonization Process." Journal of Environmental Management 109 (2012): 61-69. Web.

RCO. "Salmon Species Listed Under the Federal Endangered Species Act." Salmon Recovery. Washington State Recreation and Conservation Office. Web. 10 Mar. 2016.

Shaheen, Donald G. Contributions of Urban Roadway Usage to Water Pollution. Washington: Office of Research and Development, U.S. Environmental Protection Agency, 1975. Print.

Silvertooth, Jason R. Evaluation of Copper Removal from Stormwater Runoff Using Compost and Apatite II. Thesis. Oregon State University, 2014. Print.

SOS. "How Is Biochar Made?" Sustainable Obtainable Solutions. Web. 10 Mar. 2016.

Stevens, Donald G. Survival and Immune Response of Coho Salmon Exposed to Copper. Corvallis, OR: Environmental Protection Agency, Office of Research and Development, Corvallis Environmental Research Laboratory, Western Fish Toxicology Station, 1977. Print.

Tong, Xue-Jiao, Jiu-Yu Li, Jin-Hua Yuan, and Ren-Kou Xu. "Adsorption of Cu(II) by Biochars Generated from Three Crop Straws." Chemical Engineering Journal 172.2-3 (2011): 828-34. Web.

USBI. "Biochar Introduction." Biochar Information. US Biochar Initiative. Web. 12 Mar. 2016.

Wang, Lu, Herbert M. Espinoza, and Evan P. Gallagher. "Brief Exposure to Copper Induces Apoptosis and Alters Mediators of Olfactory Signal Transduction in Coho Salmon." Chemosphere 93.10 (2013): 2639-643. Web.

Zhang, Jie, Jia Liu, and Rongle Liu. "Effects of Pyrolysis Temperature and Heating Time on Biochar Obtained from the Pyrolysis of Straw and Lignosulfonate." Bioresource Technology 176 (2015): 288-91. Web.

Zhang, Youchi, and Wensui Luo. "Adsorptive Removal of Heavy Metal from Acidic Wastewater with Biochar Produced from Anaerobically Digested Residues: Kinetics and Surface Complexation Modeling." BioResources 9.2 (2014). Web.

7. APPENDIX

Table 7.1-Estimate isotherm constants using the linearized Langmuir and Freundlich model equations.

Initial Estimated Isotherm Constants			
Langmuir			
Biochar	q_{max} **(mg/g)**	K **(L/mg)**	R^2
D300	-0.54	-0.72	0.6505
D500	2.29	2.03	0.9612
D700	0.89	75.26	0.9052
H300	0.55	21.56	0.8656
H500	1.88	18.01	0.8217
H700	2.61	15.56	0.7791
H500 SRNOM	16.21	0.16	0.1128
H700 SRNOM	-0.26	-9.52	0.0174
Freundlich			
Biochar	n	K_f	R^2
D300	-2500	0.14	0.0089
D500	2.21	1.57	0.9607
D700	3.55	1.23	0.878
H300	2.82	0.7	0.9216
H500	1.21	7.37	0.9665
H700	1.11	13.42	0.9755
H500 SRNOM	1.03	2.21	0.9908
H700 SRNOM	0.90	3.66	0.7414

Table 7.2-Average final pH measurements for all batch isotherm experiments

Biochar	Date Tested	Final Average pH	Standard Deviation
D300	8/4/2014	6.04	0.349
	9/10/2015	6.13	0.238
D500	7/25/2014	6.02	0.587
D700	8/4/2014	6.20	0.245
	8/14/2015	6.54	0.129
H300	8/4/2014	6.43	0.138
H500	8/4/2014	6.60	0.144
	8/14/2015	7.98	0.282
H500 SRNOM	8/28/2014	6.72	0.265
H700	8/4/2014	7.15	0.335
	8/14/2015	8.80	0.124
H700 SRNOM	8/25/2014	7.37	0.308
GAC	7/31/20112	6.56	0.131

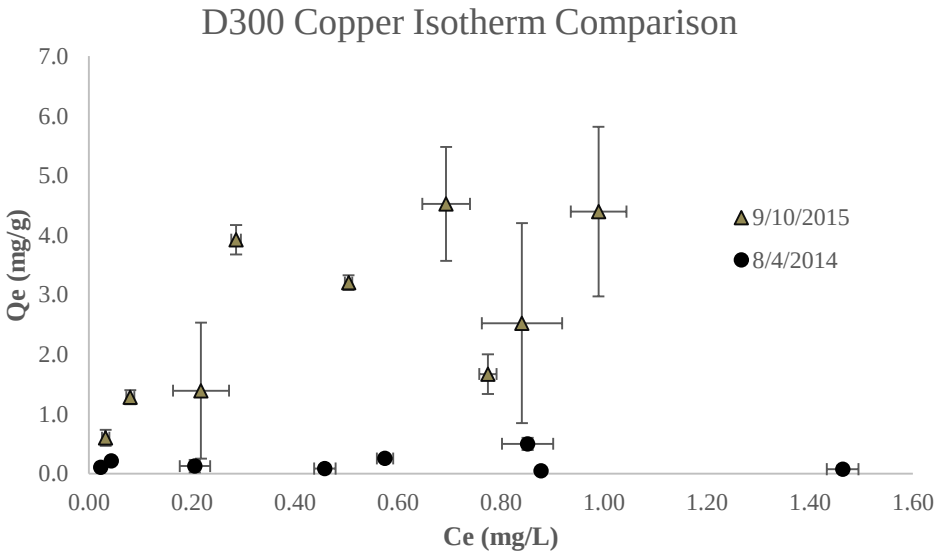

Figure 7.1- Adsorption data for D300 biochar from 08/04/2014 (initial test) and 09/10/2015 (secondary test)

Table 7.3- D300 data for 08/04/2014 isotherm experiement

D300 Isotherm Experiment (08/04/2014) Summary				
Ci (ppb)	**Ce (mg/L)**		**Qe (mg/g)**	
-	**Average**	**StDev**	**Average**	**StDev**
75	0.023	0.0081	0.104	0.0172
150	0.043	0.0055	0.212	0.0110
300	0.206	0.0294	0.125	0.1062
500	0.458	0.0207	0.083	0.0412
700	0.575	0.0158	0.254	0.0311
900	0.878	0.0040	0.045	0.0077
1100	0.852	0.0496	0.499	0.1028
1500	1.463	0.0306	0.072	0.0598

Table 7.4-D300 data for 09/10/2015 isotherm experiment

D300 Isotherm Experiment 09/10/2015 Summary				
Ci (ppb)	**Ce (mg/L)**		**Qe (mg/g)**	
-	**Average**	**StDev**	**Average**	**StDev**
75	0.032	0.0070	0.601	0.1341
150	0.080	0.0076	1.281	0.1181
300	0.217	0.0544	1.391	1.1398
500	0.286	0.0092	3.922	0.2482
700	0.504	0.0070	3.205	0.1232
900	0.775	0.0170	1.669	0.3326
1100	0.693	0.0461	4.522	0.9554
1300	0.989	0.0541	4.393	1.4214
1500	0.841	0.0780	2.521	1.6769

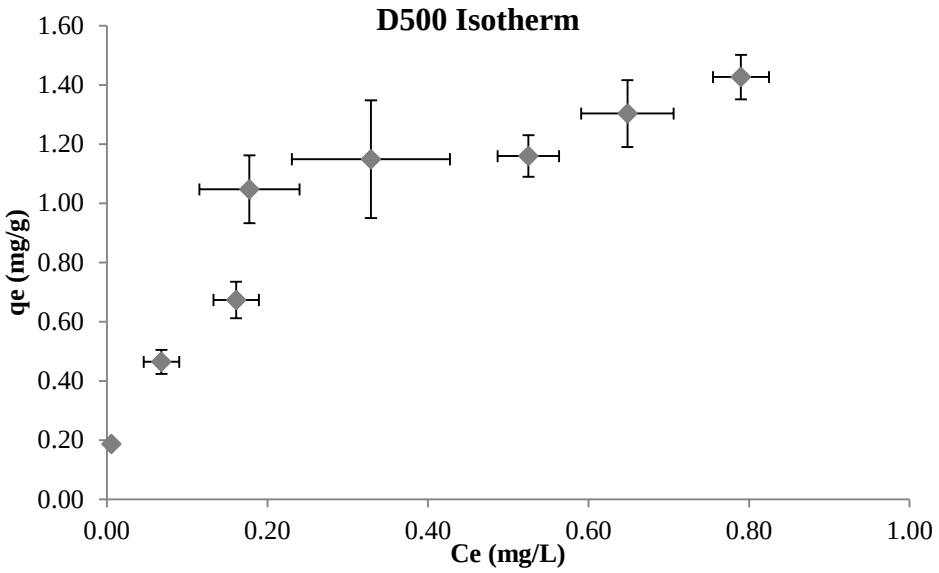

Figure 7.2- D500 isothherm data

Table 7.5- D500 isotherm data summary

D500 Isotherm Summary				
Ci (ppb)	**Ce (mg/L)**		**Qe (mg/g)**	
-	**Average**	**StDev**	**Average**	**StDev**
100	0.006	0.0012	0.19	0.0015
300	0.068	0.0222	0.46	0.0409
500	0.161	0.0283	0.67	0.0618
700	0.178	0.0623	1.05	0.1148
900	0.329	0.0983	1.15	0.1987
1100	0.525	0.0383	1.16	0.0700
1300	0.648	0.0576	1.30	0.1130
1500	0.790	0.0351	1.43	0.0755

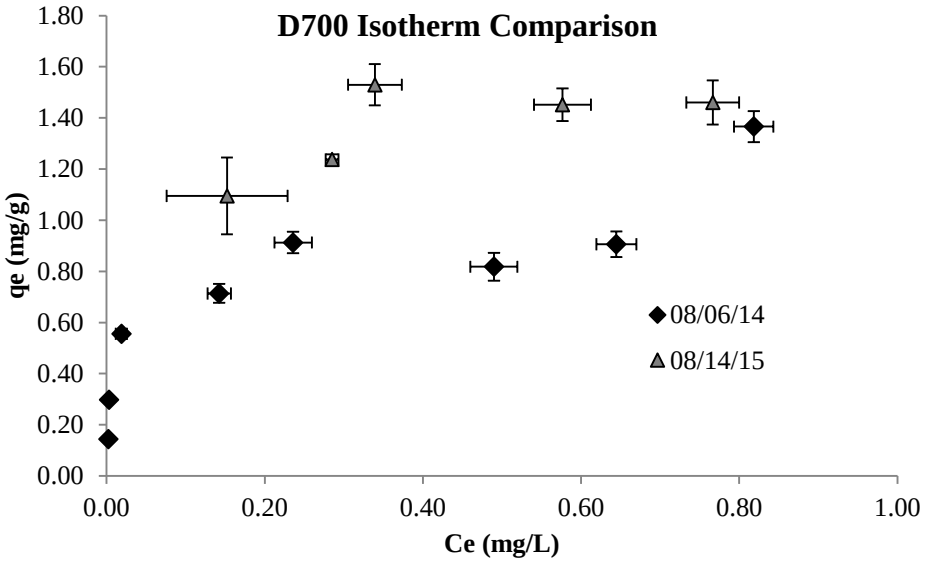

Figure 7.3- D700 isotherm data from 08/06/14 (initial test) and 08/14/15 (second test)

Table 7.6- D700 isotherm data summary from 08/06/2014

D700 Isotherm (08/06/2014) Summary				
Ci (ppb)	**Ce (mg/L)**		**Qe (mg/g)**	
-	**Average**	**StDev**	**Average**	**StDev**
75	0.002	0.0006	0.14	0.0014
150	0.003	0.0001	0.30	0.0011
300	0.019	0.0070	0.56	0.0099
500	0.142	0.0148	0.71	0.0366
700	0.236	0.0236	0.91	0.0416
900	0.490	0.0297	0.82	0.0543
1100	0.645	0.0251	0.91	0.0496
1500	0.818	0.0248	1.37	0.0608

Table 7.7-D700 isotherm data summary from 08/14/2015

D700 Isotherm (08/14/2015) Summary				
Ci (ppb)	**Ce (mg/L)**		**Qe (mg/g)**	
-	**Average**	**StDev**	**Average**	**StDev**
700	0.152	0.0764	1.10	0.1501
900	0.285	0.0080	1.24	0.0197
1100	0.339	0.0341	1.53	0.0809
1300	0.576	0.0362	1.45	0.0640
1500	0.766	0.0334	1.46	0.0860

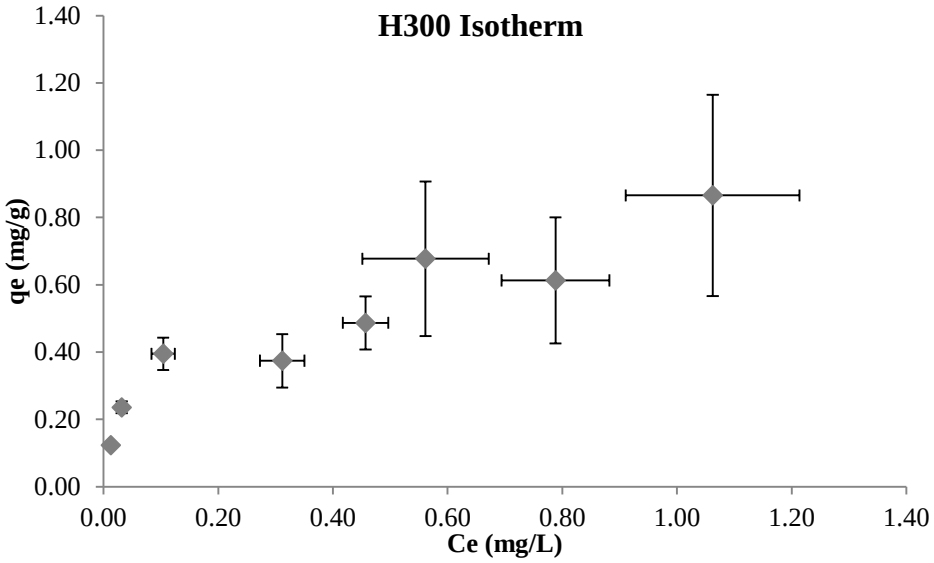

Figure 7.4- H300 isotherm data

Table 7.8-H300 isotherm data summary

H300 Isotherm Summary				
Ci (ppb)	**Ce (mg/L)**		**Qe (mg/g)**	
-	**Average**	**StDev**	**Average**	**StDev**
75	0.013	0.0011	0.12	0.0036
150	0.032	0.0066	0.24	0.0176
300	0.104	0.0206	0.39	0.0477
500	0.312	0.0386	0.37	0.0793
700	0.457	0.0396	0.49	0.0790
900	0.561	0.1104	0.68	0.2295
1100	0.788	0.0940	0.61	0.1870
1500	1.062	0.1515	0.87	0.2994

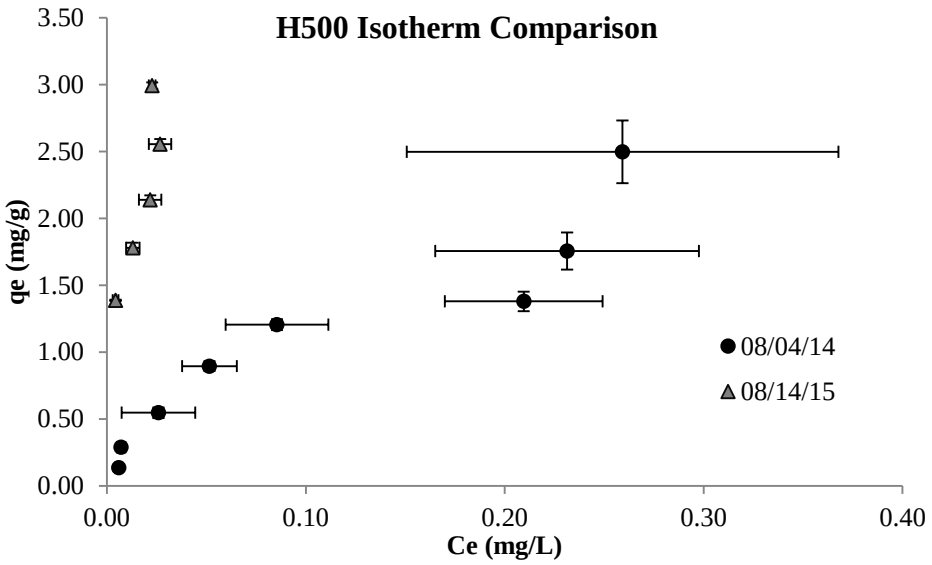

Figure 7.5-H500 isotherm comparison with data from 08/04/14 (initial test) and 08/14/2015 (second test)

Table 7.9- H500 isotherm data summary from 08/04/2014

H500 Isotherm (08/04/2014) Summary				
Ci (ppb)	**Ce (mg/L)**		**Qe (mg/g)**	
-	**Average**	**StDev**	**Average**	**StDev**
75	0.006	0.0017	0.14	0.0021
150	0.007	0.0021	0.29	0.0037
300	0.026	0.0184	0.55	0.0393
500	0.052	0.0138	0.90	0.0371
700	0.085	0.0258	1.21	0.0398
900	0.210	0.0396	1.38	0.0727
1100	0.231	0.0663	1.76	0.1383
1500	0.259	0.1085	2.50	0.2343

Table 7.10- H500 isotherm data summary from 08/14/2015

H500 Isotherm (08/14/2015) Summary				
Ci (ppb)	**Ce (mg/L)**		**Qe (mg/g)**	
-	**Average**	**StDev**	**Average**	**StDev**
700	0.004	0.0015	1.39	0.0043
900	0.013	0.0034	1.78	0.0399
1100	0.022	0.0056	2.14	0.0328
1300	0.027	0.0056	2.56	0.0366
1500	0.023	0.0017	2.99	0.0249

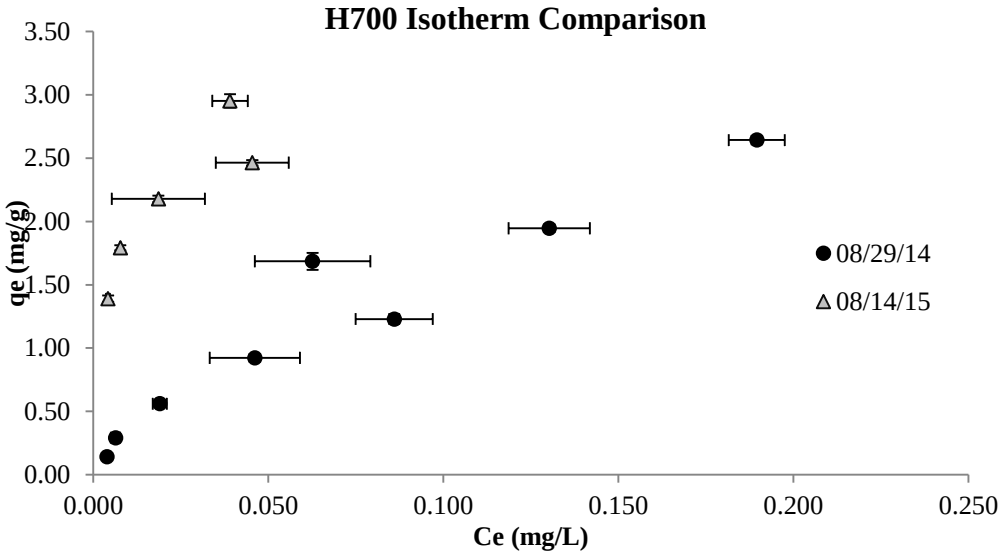

Figure 7.6- H700 isotherm comparison with data from 08/29/14 (initial test) and 08/14/2015 (second test)

Table 7.11- H500 isotherm data summary from 08/29/2014

H700 Isotherm (08/29/2014) Summary				
Ci (ppb)	**Ce (mg/L)**		**Qe (mg/g)**	
-	**Average**	**StDev**	**Average**	**StDev**
75	0.004	0.0007	0.14	0.0021
150	0.006	0.0013	0.29	0.0047
300	0.019	0.0020	0.56	0.0123
500	0.046	0.0129	0.92	0.0299
700	0.086	0.0110	1.23	0.0397
900	0.063	0.0165	1.69	0.0671
1100	0.130	0.0116	1.95	0.0303
1500	0.190	0.0080	2.64	0.0343

Table 7.12- H500 isotherm data summary from 08/14/2015

H700 Isotherm (08/14/2015) Summary				
Ci (mg/L)	**Ce (mg/L)**		**Qe (mg/g)**	
Nominal	**Average**	**StDev**	**Average**	**StDev**
700	0.004	0.0005	1.39	0.02537
900	0.008	0.0000	1.79	0.02136
1100	0.019	0.0133	2.18	0.02565
1300	0.045	0.0104	2.46	0.02148
1500	0.039	0.0051	2.95	0.05304

Table 7.13-H500 SRNOM isotherm data summary

H500 SRNOM Isotherm Summary				
Ci (ppb)	**Ce (mg/L)**		**Qe (mg/g)**	
-	**Average**	**StDev**	**Average**	**StDev**
75	0.033	0.0015	0.08	0.0028
150	0.067	0.0026	0.17	0.0048
300	0.134	0.0051	0.33	0.0110
500	0.234	0.0025	0.53	0.0122
700	0.318	0.0079	0.75	0.0198
900	0.396	0.0215	1.01	0.0419
1100	0.492	0.0255	1.21	0.0574
1500	0.696	0.0871	1.61	0.1545

Table 7.14-H700 SRNOM isotherm data summary

H700 SRNOM Isotherm Summary				
Ci (ppb)	**Ce (mg/L)**		**Qe (mg/g)**	
-	**Average**	**StDev**	**Average**	**StDev**
75	0.039	0.0008	0.07	0.0023
150	0.080	0.0046	0.14	0.0098
300	0.099	0.0106	0.40	0.0250
500	0.209	0.0127	0.58	0.0306
700	0.307	0.0196	0.77	0.0345
900	0.393	0.0150	1.01	0.0236
1100	0.503	0.0137	1.19	0.0217
1500	0.219	0.0819	2.57	0.1912

Table 7.15-GAC isotherm data summary

GAC Isotherm Summary				
Ci (ppb)	**Ce (mg/L)**		**Qe (mg/g)**	
-	**Average**	**StDev**	**Average**	**StDev**
100	0.010	0.0033	0.18	0.0066
300	0.058	0.0142	0.48	0.0283
500	0.095	0.0056	0.81	0.0113
700	0.190	0.0429	1.02	0.0857
900	0.344	0.0034	1.11	0.0068
1100	0.399	0.0146	1.40	0.0292
1300	0.615	0.0518	1.37	0.1036
1500	0.616	0.0992	1.77	0.1984

Table 7.16-Kinetics test pH measurements

	H700		**H500**		**H300**		**D300**	
Time (hrs)	**500 ppb**	**1000 ppb**	**500 ppb**	**1000 ppb**	**500 ppb**	**1000 ppb**	**500 ppb**	**1000 ppb**
0	5.98	6.03	5.97	5.99	6.04	5.96	6.05	6.01
0.25	6.13	6.21	6.09	6.07	6.25	6.40	6.40	6.31
0.5	6.22	6.17	6.11	6.14	6.21	6.35	6.44	6.26
0.75	6.27	6.31	6.23	6.15	6.22	6.31	6.46	6.30
1	6.34	6.35	6.27	6.18	6.27	6.27	6.39	6.28
2	6.31	6.14	6.27	6.24	6.28	6.33	6.30	6.25
4	6.29	6.33	6.34	6.43	6.34	6.27	6.38	6.27
8	6.32	6.40	6.39	6.38	6.43	6.49	6.48	6.32
12	6.44	6.33	6.58	6.26	6.45	6.39	6.46	6.21
36	6.61	6.34	6.52	6.53	6.60	6.26	6.49	6.14
48	6.58	6.33	5.54	6.46	6.47	6.41	6.42	6.04

Table 7.17- pH measured for large scale kinetics tests conducted on H700 biochar

	pH Measured	
Time	**11/11/2013**	**3/6/2014**
0	6.18	6.04
0.25	-	8.34
0.5	6.72	8.50
1	6.70	8.39
2	6.46	8.42
4	-	8.22
6	6.58	-
8	6.56	7.93
12	5.59	7.90
24	6.75	8.32
36	6.69	7.76
48	6.74	7.88
60	-	7.57
72	-	7.10

Table 7.18- pH measurements taken for biochar slurries tested in duplicate.

Sample	**pH**
H700 #1	8.53
H700 #2	8.48
H500 #1	9.54
H500 #2	9.55
H300 #1	8.07
H300 #2	8.08
D700 #1	7.77
D700 #2	7.44
D500 #1	6.76
D500 #2	6.47
D300 #1	4.36
D300 #2	4.38

TABLE S-1: Assignment of characteristic vibrations to individual peaks in wood and grass char ATR FT-IR spectra.

Wavenumber [cm^{-1}]	Characteristic vibrations	Functionality
3665	'free' O-H stretching	alcoholic and phenolic -OH, not hydrogen bonded (*39*) (*40*)
3200-3500	O-H stretching	water, H-bonded hydroxyl (-OH) groups (*39*) (*40*)
3200	C-H stetching	5-membered N/O-heterocyclic C (e.g., furans and pyrroles) (*22*)
3050	C-H stretching	substituted aromatic C (*22*)
2935	asymmetric C-H stretching	aliphatic CH_x (*41*)
2885	symmetric C-H stretching	aliphatic CH_x (*41*)
1740-1700	C=O stretching	mainly carboxyl (*20*); traces of aldehydes, ketones and esters (*42*) (*43*)
1600	C=C stretching	aromatic components (*20*) (*44, 45*)
	C=O stretching	C=O of conjugated ketons and quinones (*20*) (*44, 45*)
1510	C=C stretching	aromatic skeletal vibrations, indicative of lignin (*44, 45*) (*46*)
1440	C=C stretching	aromatic C, indicative of lignin, appears when bound to unsaturated group (*44, 45*) (*46*)
	α-C-H_2 bending	aliphatic -CH_2 deformations (*40*), associated with lignin and carbohydrates (*47*)
1375	O-H bending	in plane bending of phenolic -OH (*48*), related to ligneous syringyl units (*46*)
	α-C-H_3 bending	aliphatic -CH_3 deformations (*20*) (*44, 45*)
1270-1250	C-O stretching	C-O-C groups and aryl ethers (*40*) (*20*); phenolic C-O indicative of guaiacyl units associated with lignin (*46*) (*49*)
1185-1160	(asymmetric) "	C-O-C ester groups in cellulose and hemicellulose (*24*) (*47*)
1110	(symmetric) "	C-O-C stretching vibrations in cellulose and hemicellulose [j]; aliphatic -OH (*39*)
1030	"	acid derivatives, aliphatic C-O-C, and -OH representative of oxygenated functional groups of cellulose and hemicellulose (*43*) (*47*); methoxy groups of lignins (*49*)
1200-1000	C-H deformation	vibrations typical for substituted aromatics (*24*)
885, 815, 750	C-H bending	aromatic CH out-of-plane deformation (*44, 45*); less substituted rings appear at lower wavenumbers (*39*)

233

Figure 7.7-EPA FTIR spectra interpretation guide